ミノ酸を培地に添加しその影響を解析できるようになり，非代償性肝硬変では健常人と比較して樹状細胞自体の成熟化が抑制されているだけでなく細胞外のアミノ酸環境が樹状細胞の成熟化を抑制することを明らかにした(図6)[13]．しかしそれでも生体内においては食事，体内水分量，さらにその局在(末梢血，門脈血，各種臓器・リンパ節など)により細胞外のアミノ酸濃度は異なるためその点を考慮しなければならない．

5 おわりに

前向き研究によりBCAA製剤は，肝硬変患者に対して肝不全イベントの低下，QOLの改善，さらに発癌リスクを低下させる効果を持つことが報告され[28,29]，臨床試験でのBCAAの有効性が証明されている．また近年，本多らにより肝細胞自体のインターフェロンシグナルを改善させる効果も報告された[30]．慢性C型肝炎・肝硬変患者の高齢化により，副作用の少ない栄養療法の重要性が増していくことは明白である．遊離アミノ酸の免疫細胞に与える影響がより詳細に解析されれば，①感染症予防，②発癌抑制，③C型肝硬変患者のインターフェロン奏効率向上につながる可能性がある．

文 献

1) Morgan MY, Marshall AW, Milsom JP et al : Plasma amino-acid patterns in liver disease. Gut 23 : 362–370, 1982
2) Morgan MY, Milsom JP, Sherlock S : Plasma ratio of valine, leucine and isoleucine to phenylalanine and tyrosine in liver disease. Gut 19 : 1068–1073, 1978
3) Kim DH, Sarbassov DD, Ali SM et al : mTOR interacts with raptor to form a nutrient-sensitive complex that signals to the cell growth machinery. Cell 110 : 163–175, 2002
4) Kimball SR, Shantz LM, Horetsky RL et al : Leucine regulates translation of specific mRNAs in L6 myoblasts through mTOR-mediated changes in availability of eIF4E and phosphorylation of ribosomal protein S6. J Biol Chem 274 : 11647–11652, 1999
5) Tremblay F, Marette A : Amino acid and insulin signaling via the mTOR/p70 S6 kinase pathway. A negative feedback mechanism leading to insulin resistance in skeletal muscle cells. J Biol Chem 276 : 38052–38060, 2001
6) Ohtani M, Nagai S, Kondo S et al : Mammalian target of rapamycin and glycogen synthase kinase 3 differentially regulate lipopolysaccharide-induced interleukin-12 production in dendritic cells. Blood 112 : 635–643, 2008
7) Weichhart T, Costantino G, Poglitsch M et al : The TSC-mTOR signaling pathway regulates the innate inflammatory response. Immunity 29 : 565–567, 2008
8) Yaqoob P, Calder PC : Glutamine requirement of proliferating T lymphocytes. Nutrition 13 : 646–651, 1997
9) Newsholme P : Why is L-glutamine metabolism important to cells of the immune system in health, postinjury, surgery or infection? J Nutr 131 : 2515S–2522S; discussion 2523S–2524S, 2001
10) Nicklin P, Bergman P, Zhang B et al : Bidirectional transport of amino acids regulates mTOR and autophagy. Cell 136 : 521–534, 2009
11) Kakazu E, Kanno N, Ueno Y et al : Extracellular branched-chain amino acids, especially valine, regulate maturation and function of monocyte-derived dendritic cells. J Immunol 179 : 7137–7146, 2007
12) Nakamura I, Ochiai K, Imai Y et al : Restoration of innate host defense responses by oral supplementation of branched-chain amino acids in decompensated cirrhotic patients. Hepatol Res 37 : 1062–1067, 2007
13) Kakazu E, Ueno Y, Kondo Y et al : Branched chain amino acids enhance the maturation and function of myeloid dendritic cells ex vivo in patients with advanced cirrhosis. Hepatology 50 : 1936–1945, 2009
14) Mellor AL, Munn DH : IDO expression by dendritic cells: tolerance and tryptophan catabolism. Nat Rev Immunol 4 : 762–774, 2004
15) Munn DH, Sharma MD, Baban B et al : GCN2 kinase in T cells mediates proliferative arrest

and anergy induction in response to indoleamine 2,3-dioxygenase. Immunity 22 : 633–642, 2005
16) 東谷光庸，考藤達哉，黒田将子，他：C型慢性肝炎患者樹状細胞による制御性T細胞の誘導機序ートリプトファン代謝酵素（IDO）の意義. 肝臓 52：A173, 2011
17) Morris SM Jr : Arginine: master and commander in innate immune responses. Sci Signal 3 : pe27, 2010
18) Mieulet V, Yan L, Choisy C et al : TPL-2-mediated activation of MAPK downstream of TLR4 signaling is coupled to arginine availability. Sci Signal 3 : ra61, 2010
19) Sato H, Tamba M, Ishii T et al : Cloning and expression of a plasma membrane cystine/glutamate exchange transporter composed of two distinct proteins. J Biol Chem 274 : 11455–11458, 1999
20) Angelini G, Gardella S, Ardy M et al : Antigen-presenting dendritic cells provide the reducing extracellular microenvironment required for T lymphocyte activation. Proc Natl Acad Sci USA 99 : 1491–1496, 2002
21) D'Angelo JA, Dehlink E, Platzer B et al : The cystine/glutamate antiporter regulates dendritic cell differentiation and antigen presentation. J Immunol 185 : 3217–3226, 2010
22) Byl B, Roucloux I, Crusiaux A et al : Tumor necrosis factor alpha and interleukin 6 plasma levels in infected cirrhotic patients. Gastroenterology 104 : 1492–1497, 1993
23) Tilg H, Wilmer A, Vogel W et al : Serum levels of cytokines in chronic liver diseases. Gastroenterology 103 : 264–274, 1992
24) Galbois A, Thabut D, Tazi KA et al : Ex vivo effects of high-density lipoprotein exposure on the lipopolysaccharide-induced inflammatory response in patients with severe cirrhosis. Hepatology 49 : 175–184, 2009
25) Guarner C, Gonzalez-Navajas JM, Sanchez E et al : The detection of bacterial DNA in blood of rats with CCl4-induced cirrhosis with ascites represents episodes of bacterial translocation. Hepatology 44 : 633–639, 2006
26) Munoz L, Albillos A, Nieto M et al : Mesenteric Th1 polarization and monocyte TNF-alpha production: first steps to systemic inflammation in rats with cirrhosis. Hepatology 42 : 411–419, 2005
27) Ubeda M, Munoz L, Borrero MJ et al : Critical role of the liver in the induction of systemic inflammation in rats with preascitic cirrhosis. Hepatology 52 : 2086–2095, 2010
28) Marchesini G, Bianchi G, Merli M et al : Nutritional supplementation with branched-chain amino acids in advanced cirrhosis: a double-blind, randomized trial. Gastroenterology 124 : 1792–1801, 2003
29) Muto Y, Sato S, Watanabe A et al : Overweight and obesity increase the risk for liver cancer in patients with liver cirrhosis and long-term oral supplementation with branched-chain amino acid granules inhibits liver carcinogenesis in heavier patients with liver cirrhosis. Hepatol Res 35 : 204–214, 2006
30) Honda M, Takehana K, Sakai A et al : Malnutrition Impairs Interferon Signaling Through mTOR and FoxO Pathways in Patients With Chronic Hepatitis C. Gastroenterology 141 : 128–140, 2011

*　　*　　*

MAJOR ARTICLE

Hepatitis B Virus Replication Could Enhance Regulatory T Cell Activity by Producing Soluble Heat Shock Protein 60 From Hepatocytes

Yasuteru Kondo,[1] Yoshiyuki Ueno,[1] Koju Kobayashi,[2] Eiji Kakazu,[1] Masaaki Shiina,[1] Jun Inoue,[1] Keiichi Tamai,[1] Yuta Wakui,[1] Yasuhito Tanaka,[5] Masashi Ninomiya,[1] Noriyuki Obara,[1] Koji Fukushima,[1] Motoyasu Ishii,[3] Tomoo Kobayashi,[4] Hirofumi Niitsuma,[1] Satonori Kon,[2] and Tooru Shimosegawa[1]

[1]Division of Gastroenterology, Tohoku University Hospital, [2]School of Health Science, Tohoku University, [3]Department of Gastroenterology, Miyagi Social Insurance Hospital, and [4]Department of Gastroenterology, Tohoku Rosai Hospital, Sendai, and [5]Clinical Molecular Informative Medicine, Nagoya City University, Nagoya, Japan

Background. HBcAg-specific regulatory T (T_{reg}) cells play an important role in the pathogenesis of chronic hepatitis B. Soluble heat shock proteins, especially soluble heat shock protein 60 (sHSP60), could affect the function of T_{reg} cells via Toll-like receptor.

Methods. We analyzed the relationship between soluble heat shock protein production and hepatitis B virus (HBV) replication with both clinical samples from HBeAg-positive patients with chronic hepatitis B ($n = 24$) and HBeAb-positive patients with chronic hepatitis B ($n = 24$) and in vitro HBV-replicating hepatocytes. Thereafter, we examined the biological effects of sHSP60 with isolated T_{reg} cells.

Results. The serum levels of sHSP60 in patients with chronic hepatitis B were statistically significantly higher than those in patients with chronic hepatitis C ($P < .01$), and the levels of sHSP60 were correlated with the HBV DNA levels ($R = 0.532$; $P < .001$) but not with the alanine aminotransferase levels. Moreover, the levels of sHSP60 in HBV-replicating HepG2 cells were statistically significantly higher than those in control HepG2 cells. Preincubation of $CD4^+$ $CD25^+$ cells with recombinant HSP60 (1 ng/mL) statistically significantly increased the frequency of HBcAg-specific interleukin 10–secreting T_{reg} cells. The frequency of $IL7R^-CD4^+CD25^+$ cells, the expression of Toll-like receptor 2, and the suppressive function of T_{reg} cells had declined during entecavir treatment.

Conclusion. The function of HBcAg-specific T_{reg} cells was enhanced by sHSP60 produced from HBV-infected hepatocytes. Entecavir treatment suppressed the frequency and function of T_{reg} cells; this might contribute to the persistence of HBV infection.

Hepatitis B virus (HBV) is a noncytopathic DNA virus that causes chronic hepatitis and hepatocellular carcinoma as well as acute hepatitis and fulminant hepatitis [1]. HBV now affects more than 400 million people worldwide [2], and persistent infection develops in ~5% of adults and 95% of neonates who become infected with HBV.

It has been shown that the cellular immune system, including cytotoxic T lymphocytes, $CD4^+$ T helper 1 cells, and $CD4^+C25^+FoxP3^+$ regulatory T (T_{reg}) cells, plays a central role in the control of viral infection [3–6]. The hyporesponsiveness of HBV-specific T helper 1 cells and the excessive regulatory function of T_{reg} cells in peripheral blood in patients with chronic hepatitis B has been shown elsewhere [7–10]. Lamivudine treatment of chronic hepatitis B has been reported to restore both $CD4^+$ T cells and cytotoxic T lymphocyte hyporesponsiveness following the decrease of serum levels of HBV DNA and HBV-derived Ag [8, 11–13]. In our previous study, we observed that HBcAg-specific interleukin 10 (IL-10)–secreting T_{reg} cells could play an important role in the immunopathogenesis of chronic hepatitis B [9].

Received 14 July 2009; accepted 3 February 2010; electronically published 9 June 2010.

Potential conflicts of interest: none reported.

Financial support: Ministry of Health, Labor, and Welfare of Japan (Health and Labor Sciences Research Grants for the Research on Measures for Intractable Diseases); Ministry of Education, Culture, Sports, Science, and Technology of Japan (grant 21790642 to Y.K.).

Reprints or correspondence: Yoshiyuki Ueno, Division of Gastroenterology, Tohoku University Graduate School of Medicine, Seiryo 1-1, Aobaku, Sendai, 980-8574, Japan (yueno@mail.tains.tohoku.ac.jp).

The Journal of Infectious Diseases 2010;202(2):202–213

0022-1899/2010/20202-0004$15.00
DOI: 10.1086/653496

Table 1. Clinical Characteristics of Patients with Chronic Hepatitis B or Chronic Hepatitis C Included in This Study

Characteristic	Patients with chronic hepatitis B		Patients with chronic hepatitis C
	HBeAg-positive, HBeAb-negative patients	HBeAg-negative, HBeAb-positive patients	
Age, years	45.16 (12.46)	48.21 (10.23)	48.63 (7.96)
Sex, no. of patients			
Male	12	12	12
Female	12	12	12
ALT level, IU/L	76.91 (39.82)	75.96 (45.90)	76.21 (33.77)
HBV DNA level, log copies/mL	7.83 (0.86)	6.00 (0.81)	NA
Genotype, % of patients			
A	0	4.17	NA
B	12.5	8.33	NA
C	87.5	87.5	NA

NOTE. Data are mean values (standard deviations), unless otherwise indicated. ALT, alanine aminotransferase; HBV, hepatitis B virus; NA, not applicable.

Many research groups have reported the possible induction of anergy by T_{reg} cells, which constitutively express CD25 (the interleukin 2 receptor α chain) in the physiological state [14–16]. In humans, this population of T_{reg} cells, as defined by $CD4^+CD25^+CTLA4^+$ cells, $CD4^+CD25^+FoxP3^+$ cells, or $CD4^+CD25^+IL7R^-$ cells, constitutes 5%–10% of peripheral $CD4^+$ T cells and has a broad repertoire that recognizes various self and nonself antigens. It has been reported that T_{reg} cells have several different mechanisms in suppressing various kinds of immune cells [17, 18]. The important mechanisms are cell to cell contact and secretion of cytokines including IL-10 and transforming growth factor β (TGF-β) [19, 20]. HBcAg derived from HBV might induce T_{reg} cells to escape from immunological pressure, as reported in persistent infection with Epstein-Barr virus, hepatitis C virus (HCV), and human immunodeficiency virus type 1 [21–23]. Some results have indicated that reduction of HBV replication could reduce the frequency and/or function of T_{reg} cells in patients with chronic hepatitis B [4, 5, 8]. However, the key factors that affect HBcAg-specific T_{reg} cells in the replication of HBV remain unclear.

The mammalian 60-kDa heat shock protein is a many-faceted molecule. In addition to serving as a chaperone, heat shock protein 60 (HSP60) is expressed by different types of cells following their exposure to stress or immune responses and is present in the blood during inflammation [24–27]. Recently, HSP60 was reported to enhance the function of $CD4^+CD25^+$ regulatory T cell function via Toll-like receptor 2 (TLR2) signaling [28].

In this study, we investigated the serum level of HSP60 in patients with chronic hepatitis B and the relevance of HBcAg-specific IL-10-secreting T_{reg} cells and HSP60. We report evidence of the production of soluble HSP60 (sHSP60) from HBV-replicating hepatocytes, by use of clinical samples from patients with chronic hepatitis B and an in vitro HBV replication system. In addition, reductions of $CD4^+CD25^+IL7R^-$ T_{reg} cells and TLR2 expression on T_{reg} cells were observed during entecavir therapy. This study could contribute to better understanding of the immunopathogenesis of chronic hepatitis B and the development of immune-based treatment.

MATERIALS AND METHODS

Patients. Forty-eight patients with chronic hepatitis B were enrolled in this study (Table 1). The patients had serum levels of HBV DNA of >5.0 log copies/mL and had elevated alanine aminotransferase (ALT) levels (reference range, <40 IU/L) for >6 months prior to the study. To focus the analysis on the active phase of chronic hepatitis B, we excluded asymptomatic carriers and patients with immune tolerance by age (<30 years old), ALT values (<40 IU/L), and HBV DNA levels (<5.0 log copies/mL). Twenty-four patients were seropositive for HBeAg, and 24 patients were seropositive for anti-HBeAb. None of the patients tested positive for antibodies to hepatitis C virus or had liver disease due to other causes, such as alcohol, drugs, congestive heart failure, and autoimmune disease. Twenty-four patients with chronic hepatitis C and 10 healthy subjects were included as control subjects. Permission for the study was obtained from the Ethics Committee at Tohoku University Graduate School of Medicine (permission no. 2006-194]). Written informed consent was obtained from all the participants enrolled in this study. Participants were monitored for 6 months, and peripheral blood samples were obtained and assessed at 1, 2, 3, and 6 months. At each assessment, patients were evaluated for serum levels of HBV DNA, HBeAg, and anti-HBe, blood chemistry, and hematology. Levels of HBsAg, anti-HBs, total and immunoglobulin anti-HBc, HBeAg, anti-HBe, and anti–

hepatitis C virus were determined by means of commercial enzyme immunoassay kits (Abbott Laboratories). Serum levels of HBV DNA were measured by means of an Amplicor polymerase chain reaction (PCR) assay (lower limit of detection, 2.6 log copies/mL; Roche). High titers of HBV DNA were measured by means of a transcription-mediated amplification-hybridization protection assay (TMA; lower limit of detection, 3.7 log genome equivalents per milliliter). Data were adjusted by means of the following formula: Amplicor value = 0.83 × (TMA value) + 0.67.

Reagents. The following antibodies were used: CD3–allophycocyanin (APC), CD4–peridinin chlorophyll protein complex (PerCP), CD25–fluorescein isothiocyanate (FITC), CD25-phycoerythrin (PE), CD127-PE, Alexa Fluor 488 mouse anti–human CD282 (TLR2), CD284 (Toll-like receptor 4 [TLR4]), and isotype-matched control antibodies purchased from BD Bioscience. Recombinant HBcAg was obtained from Biodesign International. Recombinant HSP60 (rHSP60) was purchased from Stressgen.

Quantification of sHSP60 and soluble heat shock protein 70 (sHSP70) levels. Levels of HSP60 and heat shock protein 70 (HSP70) were quantified by use of HSP60 and HSP70 enzyme-linked immunosorbent assay (ELISA) kits (Stressgen). The serum samples from patients and supernatants from cell cultures were collected at sampling points and stocked at −20°C. The ELISA procedure was performed according to the manufacturer's protocol. First, 100-μL prepared samples were added to wells of anti-HSP60-coated plates. Then the reaction of the anti-HSP60 and horseradish peroxidase conjugate was performed after incubation and washing. Absorbance was measured at 450 nm. The HSP60 sample concentration was calculated by use of a standard curve.

Isolation of peripheral blood mononuclear cells (PBMCs) and T_{reg} cells. PBMCs were isolated from fresh heparinized blood by means of Ficoll-Hypaque density gradient centrifugation. T_{reg} cells were isolated by use of a Dynabeads regulatory $CD4^+CD25^+$ T cell kit (Invitrogen). T_{reg} cells were isolated according to the manufacturer's protocol. In brief, $CD4^+$ cells were isolated from PBMCs by means of negative selection. The remaining cells included the PBMCs depleted of $CD4^+$ cells. Then the $CD4^+CD25^+$ cells were selected positively by use of $CD25^+$ antibody combined with beads. Finally, the beads were detached by means of Detachabead (Invitrogen), because the function of T_{reg} cells might be modified by anti-CD25 antibody.

Coculture of γ-irradiated HBcAg-presenting antigen-presenting cells (APCs) and T_{reg} cells. During the isolation of T_{reg} cells, PBMCs depleted of $CD4^+$ cells could be obtained for use as APCs. PBMCs depleted of $CD4^+$ cells were stimulated at 1×10^6 cells/mL in Roswell Park Memorial Institute 1640 medium containing 10% fetal bovine serum with HBcAg (10 μg/mL) for 12 h at 37°C. Then these γ-irradiated cells were coincubated with 1×10^5 isolated T_{reg} cells that were untreated pretreated with TLR2 and TLR4 neutralizing antibody and rHSP60 (1 ng/mL) (Figures 1*A* and 2).

IL-10 secretion assay. Isolated T_{reg} cells were stimulated with HBcAg-presenting autologous γ-irradiated APCs for 12 h at 37°C. IL-10-secreting cells were stained by adding 10 μL of IL-10-detection antibody (PE-conjugated) together with anti-CD4-PerCP, anti-CD25-FITC, and anti-CD3-APC.

Flow cytometry. PBMCs were stained with CD3-APC, CD4-PerCP, CD25-FITC, and CD127-PE antibodies for 15 min on ice to analyze the frequency of $CD4^+CD25^+IL7R^-$ cells. CD4-PerCP, CD25-PE, and Alexa Fluor 488 mouse anti–human CD282 (TLR2) or CD284 (TLR4) were used for the analysis of TLR2 and TLR4 expression on $CD4^+CD25^+$ cells. Isotype-matched control antibodies were used for adjustment of the fluorescence intensity.

Construction of plasmids. The HBV plasmids was constructed as described elsewhere, with minor modifications [29]. In brief, a serum sample from one of the consecutive patients with fulminant hepatitis B (fulminant hepatitis clone 2), whose serum level of HBV DNA was the highest of the 5 patients, was used to extract total DNA (QIAamp DNA blood mini kit; Qiagen), which was subjected to nested PCR for 2 overlapping fragments; the amplified fragments were nucleotides 1051–3215/1–327 (2492 nucleotides; fragment A) and nucleotides 180–1953 (1774 nucleotides; fragment B). Then the vectors were digested with XbaI, and the XbaI-XbaI site of fragment A-pUC118 was ligated to the XbaI-XbaI site of fragment B-pUC118. Finally, a plasmid containing a 1.3-fold HBV genome (nucleotides 1051–3215/1–1953) was constructed and named pBFH2.

Cell culture and transfection. Human hepatoma HepG2 cells were incubated in Dulbecco modified Eagle medium supplemented with 10% bovine serum at 37°C and 5% carbon dioxide. For the assay of HBV replication, 6-well plates were seeded with 5×10^5 HepG2 or Huh7 cells each. On the next day, 1.5 μg of plasmid DNA were transfected to these cells by use of TransIT LT-1 transfection reagent (Mirus), and the culture supernatant and cells were collected 3 d later. The transfection efficiency was evaluated with a Great EscAPe secreted alkaline phosphatase reporter system 3 (Clontech), in which 10 ng/mL of a reporter plasmid expressing secreted alkaline phosphatase was cotransfected. Experiments were performed at least in triplicate.

Quantification of extracellular HBV DNA, HBsAg, and HBeAg levels. To digest the input plasmid DNA in the culture supernatant, 5 μL of the supernatant was treated with 5 U of DNase I (TaKaRa Bio) at 37°C for 1 h, and the reaction was stopped with edetic acid. Then total DNA was extracted with a QIAamp DNA blood mini kit, and 10 μL of 200-μL DNA solution was subjected to real-time PCR by use of a LightCycler

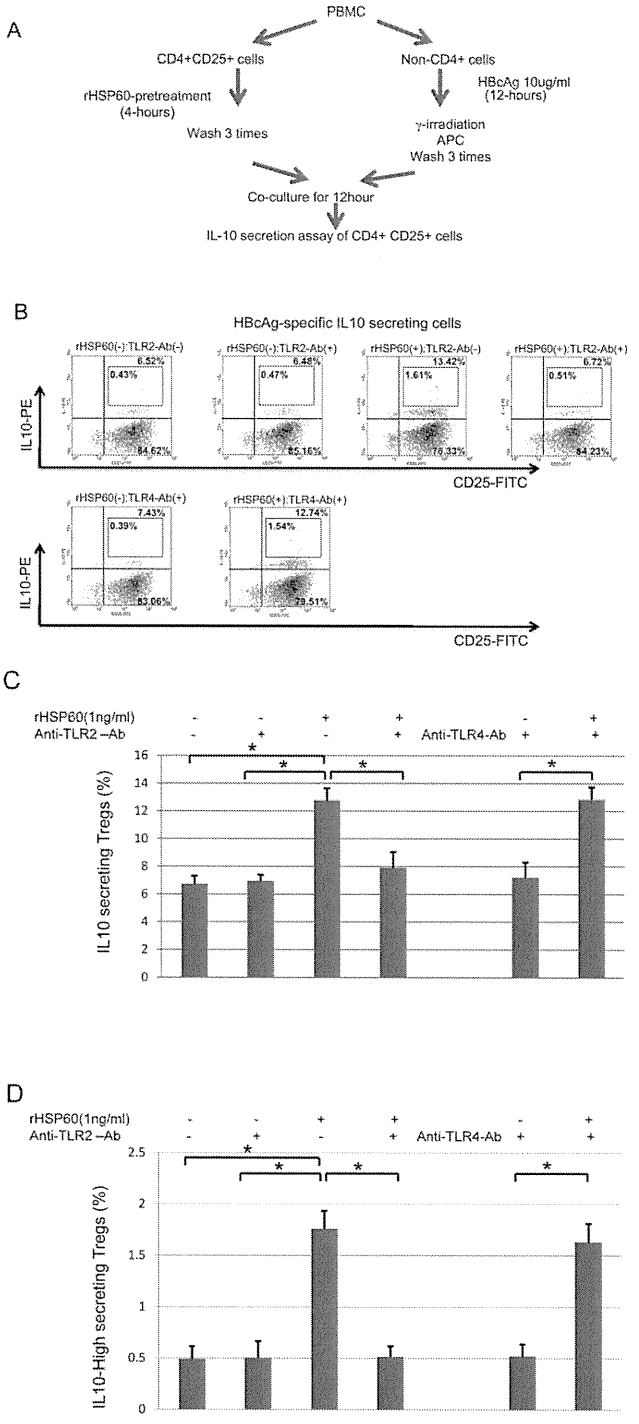

Figure 1. Effects of heat shock protein 60 (HSP60) on HBcAg-specific interleukin 10 (IL-10)–secreting regulatory T (T_{reg}) cells. *A,* Flow chart of the methods. *B,* Representative dot plots of IL-10-secreting cells in the $CD4^+CD25^+$ cells. The mixed cells (antigen-presenting cells [APCs; $CD4^-$] and isolated $CD4^+CD25^+$ cells) were stained with anti-CD4–peridinin chlorophyll protein complex (PerCP), anti-CD25–fluorescein isothiocyanate (FITC), and anti-IL-10-phycoerythrin (PE). The numbers in each top right quadrant indicate the frequencies of $CD25^+$ IL-10-secreting cells among the $CD4^+$ cells. The numbers in each bottom right quadrant indicate the frequencies of $CD4^+CD25^+IL\text{-}10^-$ cells among the $CD4^+$ cells. The numbers in each box in the top right quadrant indicate the frequencies of $CD25^+$ IL-10-secreting cells among the $CD4^+$ cells. *C,* Representative results for a sample from 1 patient with chronic hepatitis B (samples were obtained from 3 patients with chronic hepatitis B; this experiment was repeated 3 times). Bars indicate the percentage of IL-10-secreting cells among the $CD4^+$ cells with various kinds of pretreatment. *D,* Percentage of high–IL-10-secreting cells among the $CD4^+$ cells. Error bars indicate the standard deviation of 3 independent experiments with a sample from 1 patient with chronic hepatitis B. Three independent experiments yielded similar results to those shown in panels *C* and *D*. $^*P < .05$.

This figure is available in its entirety in the online version of the *Journal of Infectious Diseases.*

Figure 2. Effect of recombinant heat shock protein 60 (rHSP60) on the interleukin 10 (IL-10)–secreting activity of $CD4^+CD25^+$ cells.

system (Roche). ELISA kits were used to assay HBsAg (Hope Laboratories) and HBeAg (BioChain Institute) in 50 μL of the culture supernatant.

Sequence analysis of HBV DNA. The presence of HBV DNA in the serum samples was determined by means of PCR, as described elsewhere [30]. Nucleic acids were extracted from 100 mL of serum and subjected to nested PCR for the S gene. The amplification product of the first-round PCR was 461 bp, and that of the second-round PCR was 437 bp. The amplification products were sequenced directly on both strands by use of the BigDye Terminator Cycle Sequencing Ready reaction kit on an ABI Prism 3100 genetic analyzer (Applied Biosystems).

Carboxyfluorescein succinimidyl ester (CFSE) staining and suppression assay. The suppressive activity of regulatory T cells was analyzed by use of a CellTrace CFSE cell proliferation kit (Molecular Probes). Staining methods were followed according to the manufacturer's protocol. Briefly, the collected $CD4^+CD25^-$ cells were washed and resuspended in prewarmed phosphate-buffered saline with 0.1% bovine serum albumin at a final concentration of 3×10^5 cells/mL. CFSE solution (5 μm) was added and incubated at 37°C for 10 min. Stained cells were washed 3 times and incubated with unstained $CD4^+CD25^+$ T_{reg} cells and CD3CD28-coated stimulation beads (T cell expander) for an additional 3 d. The cells were analyzed by means flow cytometry with 488-nm excitation and emission filters.

Statistics. The data in Figures 3, 4, 1*C*, 1*D*, and 5 were analyzed by use of the independent *t* test. Statistical correlation analysis of the data in Figure 6 was performed by use of the Kendall τ_b test. The data in Figure 7 were analyzed by use of the Wilcoxon rank sum test. All of the statistical analyses were performed with SPSS software (version 10.0; SPSS). Results for which $P < .05$ were considered to be statistically significant.

RESULTS

Levels of sHSP60 and sHSP70 in samples from HBeAg-positive patients with chronic hepatitis B, HBeAg-negative patients with chronic hepatitis B, and control patients with chronic hepatitis C. The patients' characteristics, including age, sex, and ALT level, were matched among the different patient groups because the levels of sHSP60 and sHSP70 might be influenced by these factors (Table 1). The mean (± standard deviation [SD]) serum level of sHSP60 was 5.77 ± 1.19 ng/mL in HBeAg-positive patients with chronic hepatitis B, 4.12 ± 1.37 ng/mL in HBeAg-negative patients with chronic hepatitis B, 2.11 ± 0.96 ng/mL in patients with chronic hepatitis C, and 0.54 ± 0.46 ng/mL in healthy subjects. The levels of sHSP60 in patients with chronic hepatitis B (HBeAg-positive and HBeAg-negative) were statistically significantly higher than those in patients with chronic hepatitis C (Figure 3). On the other hand, the mean (± SD) serum level of sHSP70 was 7.89 ± 3.51 ng/mL in HBeAg-positive patients with chronic hepatitis B, 7.73 ± 3.71 ng/mL in HBeAg-negative patients with chronic hepatitis B, 8.09 ± 3.64 ng/mL in patients with chronic hepatitis C, and 3.54 ± 0.46 ng/mL in healthy subjects. There were no statistically significant differences in the level of sHSP70 between the chronic hepatitis B and chronic hepatitis C patient groups (Figure 3). Then we examined the correlations between the HSP60, HSP70, and HBV DNA or ALT levels. The levels of sHSP60 were correlated with the HBV DNA levels ($r = 0.532$; $P < .001$) but not with the ALT levels ($r = 0.101$; $P = .315$) (Figures 6*A* and 6*B*). On the other hand, the levels of sHSP70 were correlated with the ALT levels ($r = 0.520$; $P < .001$) but not with the HBV DNA levels ($r = 0.076$; $P < .449$) (Figure 6*C* and 6*D*).

HBV replication could directly induce sHSP60 production in vitro. Two kinds of plasmids carrying a 1.3-fold HBV genome that could replicate in HepG2 cells were used to analyze whether HBV replication could affect the production of sHSP60 in culture medium. The transfection efficiency was almost the

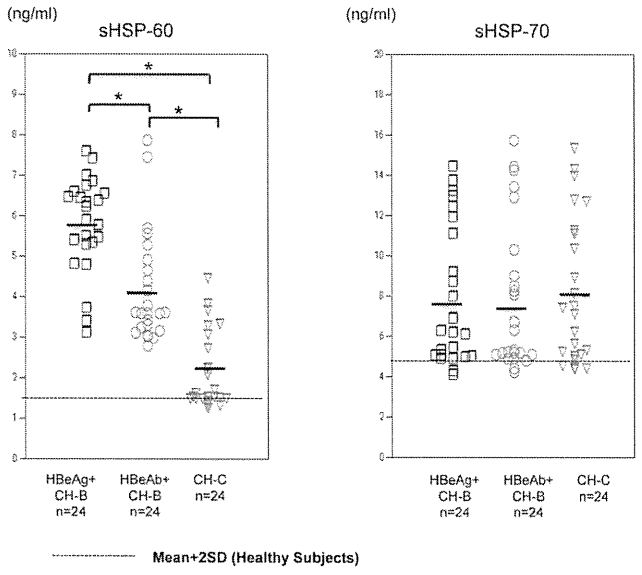

Figure 3. Quantification of serum levels of heat shock protein 60 (HSP60) and heat shock protein 70 (HSP70) in HBeAg-positive patients with chronic hepatitis B (CH-B), HBeAb-positive patients with CH-B, and patients with chronic hepatitis C (CH-C). Serum levels of HSP60 and HSP70 were quantified by means of enzyme-linked immunosorbent assay. The bar represents the means of the levels of HSP60 and HSP70. Dotted lines indicate the mean value plus 2 times the standard deviation (SD) of the levels of healthy subjects.

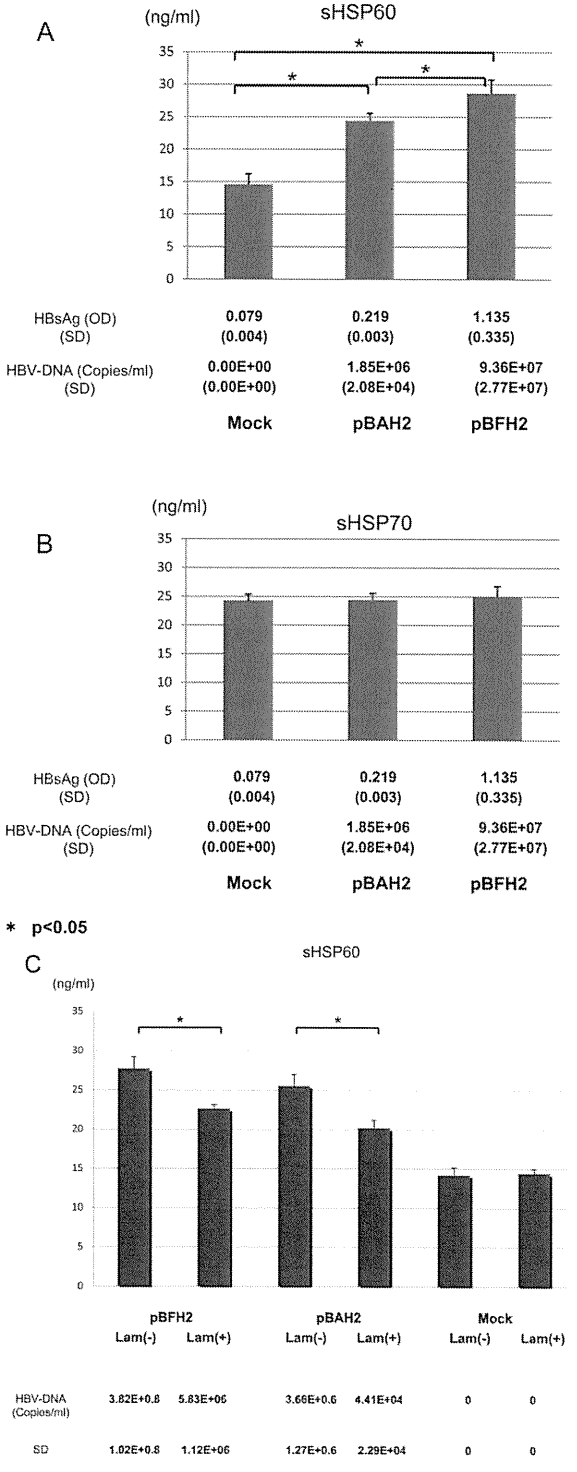

Figure 4. Direct effect of hepatitis B virus (HBV) on the production of heat shock protein 60 (HSP60) and heat shock protein 70 (HSP70). Two kinds of plasmid (pBAH2 and pBFH2) carrying a 1.3-fold HBV genome that could replicate in HepG2 cells and a mock plasmid were used to analyze whether HBV replication affects the production of soluble HSP60 (sHSP60) in culture medium. The levels of sHSP60 and soluble HSP70 (sHSP70) were compared among the 3 plasmid groups. Bars indicate the levels of HSP60 (*A*) and HSP70 (*B*). The HBsAg and HBV DNA levels and standard deviations (SDs) are included below the bar graphs. *C*, Levels of sHSP60 in cells with and those in cells without lamivudine treatment. The cells were treated with lamivudine (Lam; 0.5 μmol/L) for 72 h. Three independent experiments were performed.

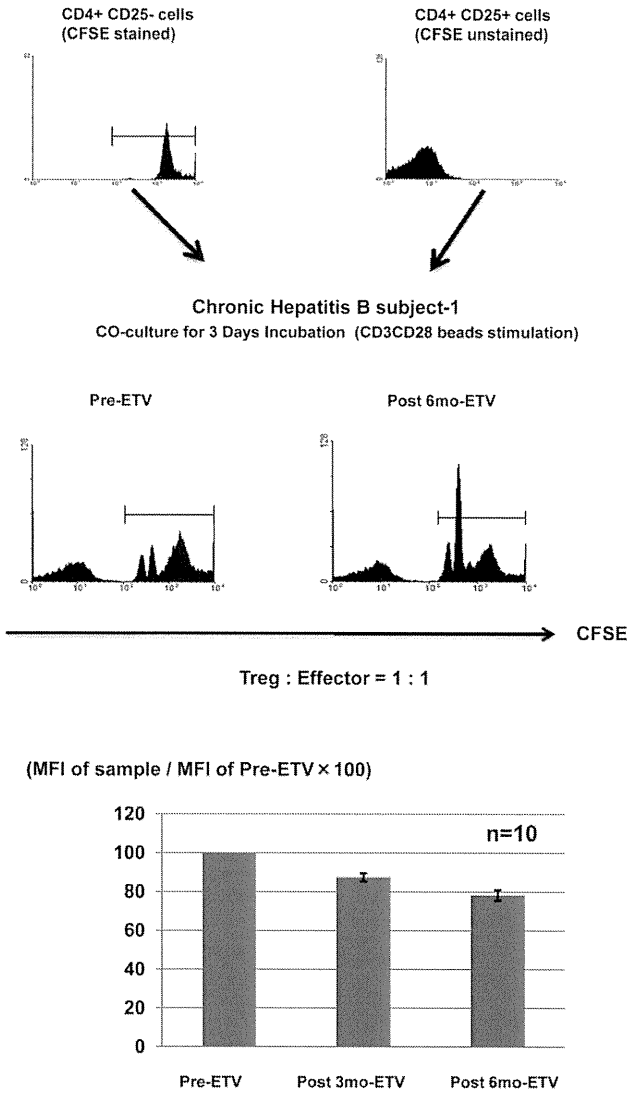

Figure 5. Suppression assay of regulatory T (T_{reg}) cells. The suppressive activity of T_{reg} cells was analyzed by means of coincubation of unstained isolated T_{reg} cells and autologous $CD4^+CD25^-$ cells with carboxyfluorescein succinimidyl ester (CFSE) staining. *A,* Representative histogram of CFSE-stained $CD4^+CD25^-$ effector cells and unstained $CD4^+CD25^+$ T_{reg} cells. *B,* Various levels of cell division in $CD4^+CD25^-$ effector cells observed 3 d after coincubation with CD3CD28-coated beads. *C,* Mean fluorescence intensity (MFI) of CFSE staining of $CD4^+CD25^-$ cells before treatment, 3 months after the start of entecavir (ETV) treatment, and 6 months after the start of entecavir treatment. The bars show the MFI of the samples divided by the MFI of the pretreatment samples ×100. The error bars indicate the standard deviations of the data.

same among the different plasmids (data not shown). The mean (± SD) HBV DNA levels of pBAH2 and pBFH2 were $1.85 \times 10^6 \pm 2.08 \times 10^4$ and $9.36 \times 10^7 \pm 2.77 \times 10^7$ copies/mL, respectively. The levels of sHSP60 in the supernatant of the pBAH2- and pBFH2-transfected HepG2 cells were statistically significantly higher than that of the mock-transfected HepG2 cells ($P < .05$) (Figure 4*A*). However, the levels of sHSP70 in the supernatant of the pBAH2- and pBFH2-transfected HepG2 cells were comparable with that of the mock-transfected HepG2 cells (Figure 4*B*). The addition of HBV-derived antigen in the culture supernatant could not increase the level of sHSP60 (data not shown). We performed the experiment on the suppression of HBV replication by nucleoside analogues in vitro. The suppression of HBV replication could statistically significantly reduce the production of sHSP60 (Figure 4*C*). These data indicate that HBV replication could increase the level of sHSP60 in the supernatant of the hepatocyte culture.

The effect of HSP60 on the HBcAg-specific IL-10-secreting T_{reg} cells. Previously, we found that HBcAg-specific IL-10-secreting cells could play an important role in the hyporesponsiveness of T cells in patients with chronic hepatitis B [9]. The effects of HSP60 on HBcAg-specific IL-10-secreting T_{reg} cells were analyzed. The appropriate dose of rHSP60 pretreatment was determined by use of PBMCs from healthy subjects (Figure 2). Pretreatment with rHSP60 could increase the frequency of HBcAg-specific IL-10-secreting cells statistically significantly ($P < .01$) and enhance the function of IL-10 secretion of HBcAg-specific T_{reg} cells, because the frequencies of high-intensity cells with IL-10 staining in HSP60 pretreatment T_{reg} cells were statistically significantly higher than those of control groups (Figure 1*D*). Moreover, these effects were completely blocked by neutralizing TLR2 antibody but not by TLR4 antibody. These data indicate that HSP60 might enhance the susceptibility and function of IL-10 secretion of HBcAg-specific T_{reg} cells.

Sequential analysis of clinical samples collected during entecavir therapy. Ten patients were selected for sequential analysis during entecavir therapy. The titers of HBV DNA and the ALT level rapidly decreased during entecavir therapy (Figures 7*A* and 7*B*). The serum levels of HSP60 had statistically significantly decreased at 3 months and at 6 months after the start of entecavir therapy. The frequency of T_{reg} cells and the expression level of TLR2 during entecavir treatment were quantified sequentially for up to 6 months during treatment by means of flow cytometry analysis. The frequency of $CD4^+CD25^+$ cells decreased, although not statistically significantly. On the other hand, the frequency of $CD4^+CD25^+IL7R^-$ cells (subpopulation of $CD4^+CD25^+$ cells) had statistically significantly decreased at 3 months and at 6 months after the start of entecavir therapy. The reason for the discrepancy could be that $CD4^+CD25^+$ cells included not only T_{reg} cells but also activated $CD4^+$ effector cells. Previously, some research groups had found that $CD4^+CD25^+FoxP3^+$ cells are almost the same as $CD4^+CD25^+IL7R^-$ cells. Therefore, our data indicate that entecavir therapy could reduce the frequency of T_{reg} cells. We also investigated the frequency of $CD4^+CD25^+FoxP3^+$ cells during lamivudine therapy (Figure 8). The frequency of

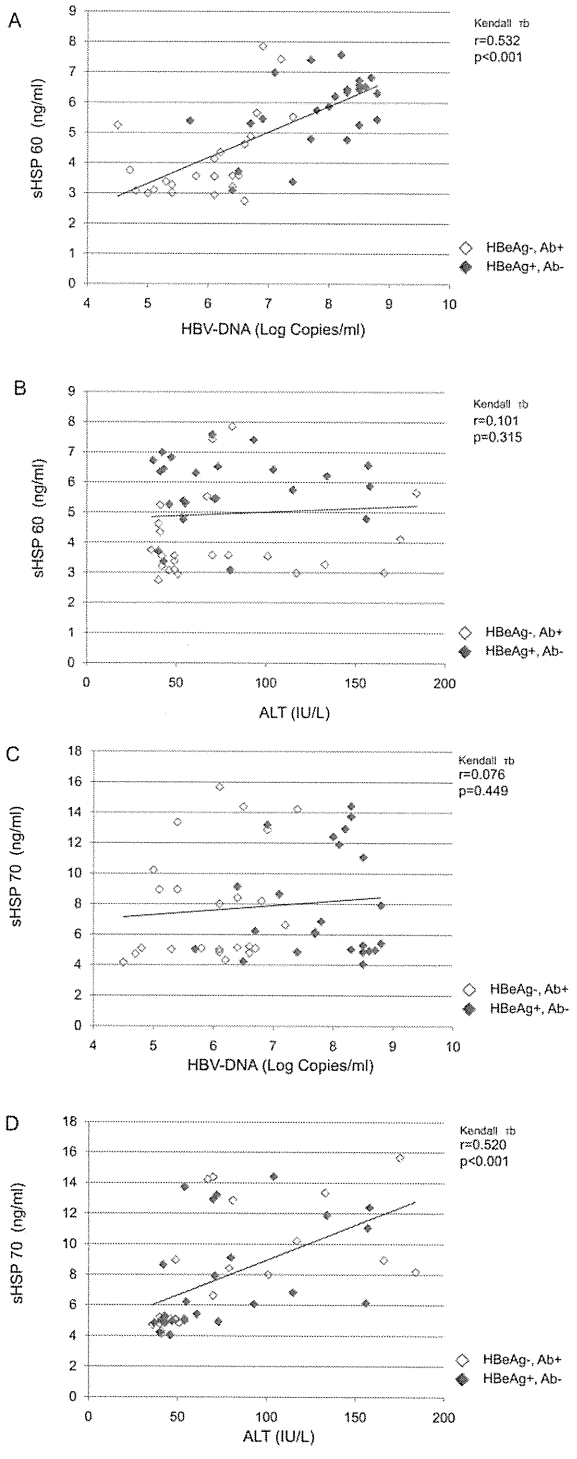

Figure 6. Analysis of the correlations between levels of heat shock proteins (HSPs), hepatitis B virus (HBV) DNA, and alanine aminotransferase (ALT). Open symbols indicate the values in samples from HBeAg-negative, HBeAb-positive patients. Filled symbols indicate the values in samples from HBeAg-positive, HBeAb-negative patients. The statistical analysis was performed by use of nonparametric Kendall τ_b methods. An approximately straight line is included in each graph. *A,* Correlation between heat shock protein 60 (HSP60) level and HBV DNA level. *B,* Correlation between HSP60 level and ALT level. *C,* Correlation between heat shock protein 70 (HSP70) level and HBV DNA level. *D,* Correlation between HSP70 level and ALT level.

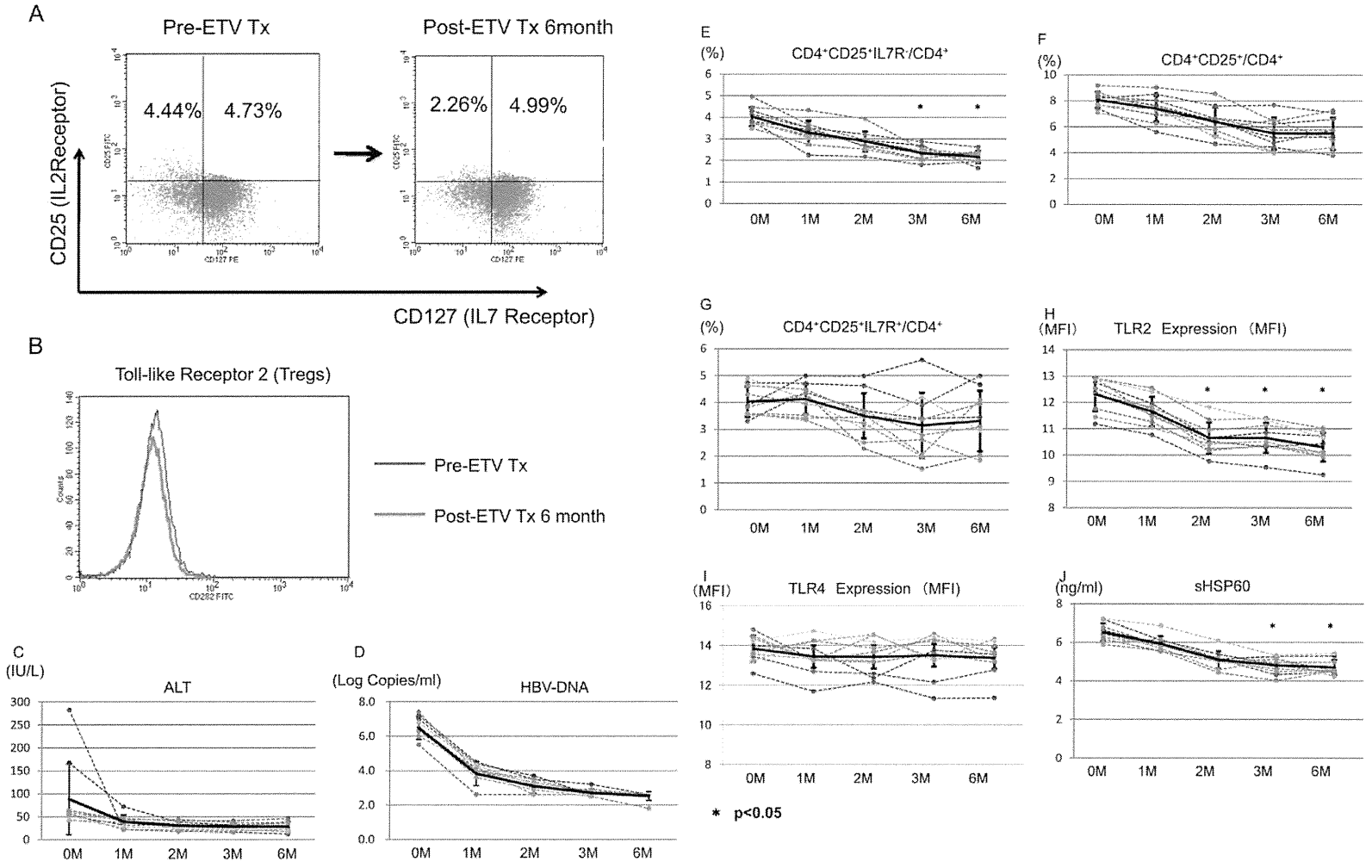

Figure 7. Sequential analysis of primary lymphocytes and soluble heat shock protein 60 (sHSP60) during entecavir (ETV) therapy. *A,* Representative dot plots of the $CD4^+CD25^+IL7R^-$ cells before treatment and 6 months after the start of treatment. Peripheral blood mononuclear cells were stained with anti-CD3, anti-CD4, anti-CD25, and anti–IL7R (CD127). The phenotypes of the $CD4^+$ cells were determined as follows: $CD4^+CD25^+IL7R^-$ cells were identified as regulatory cells and $CD4^+CD25^+IL7R^+$ cells were identified as activated $CD4^+$ cells. *B,* Representative histogram of Toll-like receptor 2 (TLR2) surface expression on $CD4^+CD25^+$ regulatory T (T_{reg}) cells before treatment and 6 months after the start of treatment. *C* and *D,* Serum levels of alanine aminotransferase (ALT) and hepatitis B virus (HBV) DNA during ETV treatment. Solid black lines and error bars indicate the mean values and standard deviations, respectively. *E–G,* Frequencies of $CD4^+CD25^+IL7R^-$cells, $CD4^+CD25^+$ cells, and $CD4^+CD25^+IL7R^+$ cells among $CD4^+$ cells during ETV treatment, respectively. *H* and *I,* Mean fluorescence intensity (MFI) of TLR2 and Toll-like receptor 4 (TLR4) expression on $CD4^+CD25^+$ cells during ETV treatment. *J,* Serum levels of sHSP60 during ETV treatment. $^*P < .01$ for comparison between pretreatment levels and posttreatment levels.

This figure is available in its entirety in the online version of the *Journal of Infectious Diseases*.

Figure 8. Frequency of $CD4^+CD25^+FoxP3^+$ cells.

$CD4^+CD25^+FoxP3^+$ cells was also decreased during lamivudine therapy. Moreover, the expression level of TLR2 on $CD4^+CD25^+$ cells gradually declined during entecavir therapy (Figure 7*G*).

Suppressive activity of T_{reg} cells. The suppressive activity of T_{reg} cells was analyzed by means of coincubation of unstained isolated T_{reg} cells and autologous $CD4^+CD25^-$ cells with CFSE staining. Ex vivo peripheral blood samples from 10 selected patients were analyzed before treatment, 3 months after the start of treatment, and 6 months after the start of treatment. The mean fluorescence intensity of the CFSE staining of the $CD4^+CD25^-$ cells was statistically significantly decreased at 6 months after the start of treatment ($P < .05$). These data indicate that the suppressive activity of T_{reg} cells was gradually decreased during entecavir treatment.

DISCUSSION

In this study, we have demonstrated that the levels of sHSP60 in patients with chronic hepatitis B were statistically significantly higher than those in patients with chronic hepatitis C. Moreover, the levels of sHSP60 were correlated with the HBV DNA levels but not with the ALT levels. On the other hand, the levels of sHSP70 were correlated with the ALT levels but not with the HBV DNA levels. This discrepancy in the correlation might be due to differences in the mechanism of heat shock protein production or secretion. The release of such heat shock proteins from cells is triggered by physical trauma and behavioral stress as well as by exposure to immunological danger signals [31, 32]. Stress protein release occurs both through physiological secretion mechanisms and during cell death by necrosis [33, 34]. HSP60 might be induced by the stress of HBV replication, because the levels of HSP60 were clearly correlated with the HBV DNA levels. On the other hand, HSP70 secretion might also be caused by cell death, because the levels of sHSP70 were correlated with the ALT levels. However, we should wait for more detailed studies about the HBV-specific induction of HSP60 to confirm this correlation. Extracellular stress proteins of the heat shock protein and glucose-regulated stress protein families, including HSP60, have powerful effects on the immune response [35]. Moreover, various kinds of immune cells such as macrophages, dendritic cells, $CD4^+$effector T cells, and T_{reg} cells are affected by heat shock proteins [28, 35]. Most recently, Cohen-Sfady et al [36] reported that HSP60 enhanced the activity of IL-10 secretion from B cells. This effect could support our findings of the immune-suppressive effect of HSP60. However, we can not draw conclusions about the whole effects of immune responses because the various kinds of immune cells might affect each other by means of cytokines, chemokines, stress-related proteins, and direct binding.

In this study, we focused on the effect of HSP60 on T_{reg} cell function by isolating T_{reg} cells, because many research groups had reported that the function and frequency of T_{reg} cells might be related to HBV replication. T_{reg} cells play an important role in the immune-hyporesponsiveness of patients with chronic hepatitis B. Previously, we demonstrated that the polarization of $CD4^+$ T cells was suppressed when the cells were stimulated with HBcAg in patients with chronic hepatitis B. T_{reg} cells are important cells in the suppression of the T helper 1 cell response by HBcAg, as demonstrated by the increased population of IL-10-secreting $CD4^+CD25^+$ cells. This indicates the presence of an inducible T_{reg} cell population, which is specific for HBcAg and produces IL-10, as well as a natural T_{reg} cell population in patients with chronic hepatitis B. Pretreatment with rHSP60 increased the frequency of HBcAg-specific IL-10-secreting $CD4^+CD25^+$ cells and enhanced the IL-10-secreting activity. These results indicate that pretreatment with rHSP60 might enhance the susceptibility of the HBcAg response and the function of IL-10 production by T_{reg} cells. These data might not imply that there was an expansion of HBcAg-specific T_{reg} cells as a result of the rHSP60 pretreatment, because the incubation phase was for only 16 h (4 h of pretreatment with rHSP60 plus 12 h of coincubation with HBcAg-presenting APCs). However, there is a possibility that continuous exposure to sHSP60 might induce an expansion of T_{reg} cells by enhancing the sensitivity of the expansion signal.

In this study, we found that the effect of HSP60 could be blocked by TLR2 neutralizing antibody but not by TLR4 neutralizing antibody. These data indicate that the effect of HSP60 could depend on TLR2. During entecavir therapy, not only the frequency of T_{reg} cells but also the serum levels of HSP60 and surface expression of TLR2 on T_{reg} cells gradually decreased. Therefore, we performed the suppression assay to detect the activity of T_{reg} cells by use of ex vivo isolated T_{reg} cells. The results of this suppression assay indicate that the reduction of the HBV DNA level could suppress the excessive activity of T_{reg} cells. In our previous study, the frequency and the function of HBV-specific cytotoxic T lymphocytes were partially recovered after therapy with nucleoside or nucleotide analogues [11]. The results clearly indicate that this restoration might be due to not only the reduction of HBV antigens but also the reduction of the frequency and function of T_{reg} cells.

On the basis of genomic analysis, 8 genotypes (A–H) of HBV have been defined, among which genotypes A, B, and especially C are prevalent in Japan [37–40]. Previous studies suggested that the clinical outcome of chronic hepatitis B was more severe in patients infected with genotype C, compared with those infected with genotype B [38, 39]. In this study, most of the

samples had HBV genotype C because of the high frequency of HBV genotype C infection in Japan. However, the expression levels of HSP60 were different among samples with the various genotypes in preliminary in vitro studies (data not shown). In addition, the expression patterns of chemokines in HBV-replicating Huh7 cells are apparently different among the various genotypes (Y. Kondo et al, unpublished data, May 2009). However, during entecavir treatment, the level of sHSP60 production in patients with genotype Bj HBV infection was quite similar to that in patients with genotype C HBV infection. We could not determine the relevance of the HBV genotypes and sHSP60 production levels because of the small numbers of genotype Bj–infected patients in this study.

In conclusion, we found that HSP60 was produced by HBV-replicating hepatocytes and determined the relevance of sHSP60 to T_{reg} cells functions, especially for IL-10-secreting activity. The understanding of the immunopathogensis of chronic hepatitis B could contribute to the development of novel kinds of immune therapy. Combination therapy with nucleoside or nucleotide analogues should be a reasonable method, because the suppression of HBV replication could reduce the excessive immune tolerance induced by T_{reg} cells.

References

1. Tiollais P, Pourcel C, Dejean A. The hepatitis B virus. Nature **1985**; 317:489–495.
2. Lai CL, Ratziu V, Yuen MF, Poynard T. Viral hepatitis B. Lancet **2003**; 362:2089–2094.
3. Kagi D, Ledermann B, Burki K, Zinkernagel RM, Hengartner H. Molecular mechanisms of lymphocyte-mediated cytotoxicity and their role in immunological protection and pathogenesis in vivo. Annu Rev Immunol **1996**; 14:207–232.
4. Peng G, Li S, Wu W, Sun Z, Chen Y, Chen Z. Circulating CD4+ CD25+ regulatory T cells correlate with chronic hepatitis B infection. Immunology **2008**; 123:57–65.
5. Barboza L, Salmen S, Goncalves L, et al. Antigen-induced regulatory T cells in HBV chronically infected patients. Virology **2007**; 368:41–49.
6. Kondo Y, Ueno Y, Shimosegawa T. Immunopathogenesis of hepatitis B persistent infection: implications for immunotherapeutic strategies. Clin J Gastroenterol **2009**; 2:71–79.
7. Xu D, Fu J, Jin L, et al. Circulating and liver resident CD4+CD25+ regulatory T cells actively influence the antiviral immune response and disease progression in patients with hepatitis B. J Immunol **2006**; 177: 739–747.
8. Manigold T, Racanelli V. T-cell regulation by CD4 regulatory T cells during hepatitis B and C virus infections: facts and controversies. Lancet Infect Dis **2007**; 7:804–813.
9. Kondo Y, Kobayashi K, Ueno Y, et al. Mechanism of T cell hyporesponsiveness to HBcAg is associated with regulatory T cells in chronic hepatitis B. World J Gastroenterol **2006**; 12:4310–4317.
10. Kondo Y, Kobayashi K, Asabe S, et al. Vigorous response of cytotoxic T lymphocytes associated with systemic activation of CD8 T lymphocytes in fulminant hepatitis B. Liver Int **2004**; 24:561–567.
11. Kondo Y, Asabe S, Kobayashi K, et al. Recovery of functional cytotoxic T lymphocytes during lamivudine therapy by acquiring multi-specificity. J Med Virol **2004**; 74:425–433.
12. Chisari FV, Ferrari C. Hepatitis B virus immunopathogenesis. Annu Rev Immunol **1995**; 13:29–60.
13. Reignat S, Webster GJ, Brown D, et al. Escaping high viral load exhaustion: CD8 cells with altered tetramer binding in chronic hepatitis B virus infection. J Exp Med **2002**; 195:1089–1101.
14. Suri-Payer E, Amar AZ, Thornton AM, Shevach EM. CD4+CD25+ T cells inhibit both the induction and effector function of autoreactive T cells and represent a unique lineage of immunoregulatory cells. J Immunol **1998**; 160:1212–1218.
15. Chen W, Jin W, Hardegen N, et al. Conversion of peripheral CD4+CD25− naive T cells to CD4+CD25+ regulatory T cells by TGF-beta induction of transcription factor Foxp3. J Exp Med **2003**; 198:1875–1886.
16. Hori S, Nomura T, Sakaguchi S. Control of regulatory T cell development by the transcription factor Foxp3. Science **2003**; 299:1057–1061.
17. Suvas S, Kumaraguru U, Pack CD, Lee S, Rouse BT. CD4+CD25+ T cells regulate virus-specific primary and memory CD8+ T cell responses. J Exp Med **2003**; 198:889–901.
18. Nakamura K, Kitani A, Fuss I, et al. TGF-beta 1 plays an important role in the mechanism of CD4+CD25+ regulatory T cell activity in both humans and mice. J Immunol **2004**; 172:834–842.
19. Zheng SG, Wang JH, Gray JD, Soucier H, Horwitz DA. Natural and induced CD4+CD25+ cells educate CD4+CD25− cells to develop suppressive activity: the role of IL-2, TGF-beta, and IL-10. J Immunol **2004**; 172:5213–5221.
20. Sundstedt A, O'Neill EJ, Nicolson KS, Wraith DC. Role for IL-10 in suppression mediated by peptide-induced regulatory T cells in vivo. J Immunol **2003**; 170:1240–1248.
21. Ulsenheimer A, Gerlach JT, Gruener NH, et al. Detection of functionally altered hepatitis C virus-specific CD4 T cells in acute and chronic hepatitis C. Hepatology **2003**; 37:1189–1198.
22. Marshall NA, Vickers MA, Barker RN. Regulatory T cells secreting IL-10 dominate the immune response to EBV latent membrane protein 1. J Immunol **2003**; 170:6183–6189.
23. Beilharz MW, Sammels LM, Paun A, et al. Timed ablation of regulatory CD4+ T cells can prevent murine AIDS progression. J Immunol **2004**; 172:4917–4925.
24. Wallin RP, Lundqvist A, More SH, von Bonin A, Kiessling R, Ljunggren HG. Heat-shock proteins as activators of the innate immune system. Trends Immunol **2002**; 23:130–135.
25. Raz I, Elias D, Avron A, Tamir M, Metzger M, Cohen IR. Beta-cell function in new-onset type 1 diabetes and immunomodulation with a heat-shock protein peptide (DiaPep277): a randomised, double-blind, phase II trial. Lancet **2001**; 358:1749–1753.
26. Hu W, Hasan A, Wilson A, et al. Experimental mucosal induction of uveitis with the 60-kDa heat shock protein-derived peptide 336–351. Eur J Immunol **1998**; 28:2444–2455.
27. Mor F, Cohen IR. T cells in the lesion of experimental autoimmune encephalomyelitis: enrichment for reactivities to myelin basic protein and to heat shock proteins. J Clin Invest **1992**; 90:2447–2455.
28. Zanin-Zhorov A, Cahalon L, Tal G, Margalit R, Lider O, Cohen IR. Heat shock protein 60 enhances CD4+ CD25+ regulatory T cell function via innate TLR2 signaling. J Clin Invest **2006**; 116:2022–2032.
29. Sugiyama M, Tanaka Y, Kato T, et al. Influence of hepatitis B virus genotypes on the intra- and extracellular expression of viral DNA and antigens. Hepatology **2006**; 44:915–924.
30. Inoue J, Takahashi M, Nishizawa T, et al. High prevalence of hepatitis delta virus infection detectable by enzyme immunoassay among apparently healthy individuals in Mongolia. J Med Virol **2005**; 76:333–340.
31. Lindquist S, Craig EA. The heat-shock proteins. Annu Rev Genet **1988**; 22:631–677.
32. Ellis RJ. The molecular chaperone concept. Semin Cell Biol **1990**; 1: 1–9.
33. Hightower LE, Guidon PT Jr. Selective release from cultured mammalian cells of heat-shock (stress) proteins that resemble glia-axon transfer proteins. J Cell Physiol **1989**; 138:257–266.
34. Mambula SS, Calderwood SK. Heat shock protein 70 is secreted from

tumor cells by a nonclassical pathway involving lysosomal endosomes. J Immunol **2006**; 177:7849–7857.
35. Calderwood SK, Mambula SS, Gray PJ Jr, Theriault JR. Extracellular heat shock proteins in cell signaling. FEBS Lett **2007**; 581:3689–3694.
36. Cohen-Sfady M, Pevsner-Fischer M, Margalit R, Cohen IR. Heat shock protein 60, via MyD88 innate signaling, protects B cells from apoptosis, spontaneous and induced. J Immunol **2009**; 183:890–896.
37. Mahmood S, Niiyama G, Kamei A, et al. Influence of viral load and genotype in the progression of hepatitis B-associated liver cirrhosis to hepatocellular carcinoma. Liver Int **2005**; 25:220–225.
38. Akuta N, Suzuki F, Kobayashi M, et al. Virological and biochemical relapse after discontinuation of lamivudine monotherapy for chronic hepatitis B in Japan: comparison with breakthrough hepatitis during long-term treatment. Intervirology **2005**; 48:174–182.
39. Kobayashi M, Suzuki F, Akuta N, et al. Response to long-term lamivudine treatment in patients infected with hepatitis B virus genotypes A, B, and C. J Med Virol **2006**; 78:1276–1283.
40. Tanaka Y, Mizokami M. Genetic diversity of hepatitis B virus as an important factor associated with differences in clinical outcomes. J Infect Dis **2007**; 195:1–4.

Am J Physiol Gastrointest Liver Physiol 299: G769–G777, 2010.
First published June 24, 2010; doi:10.1152/ajpgi.00237.2010.

Differential transcriptional characteristics of small and large biliary epithelial cells derived from small and large bile ducts

S. Glaser,[1,2]* M. Wang,[3]* Y. Ueno,[4] J. Venter,[5] K. Wang,[3] H. Chen,[3] G. Alpini,[1,2,5] and A. Holterman[3]

[1]*Scott and White Digestive Disease Research Center, and* [2]*Central Texas Veterans Health Care System, Temple, Texas;* [3]*Departments of Pediatrics and Surgery, RUSH University Medical Center, Chicago, Illinois;* [4]*Tohoku University Graduate School of Medicine, Miyagi, Japan; and* [5]*Division of Gastroenterology, Department of Medicine, College of Medicine, Texas A&M Health Science Center, College Station, Texas*

Submitted 19 May 2010; accepted in final form 16 June 2010

Glaser S, Wang M, Ueno Y, Venter J, Wang K, Chen H, Alpini G, Holterman A. Differential transcriptional characteristics of small and large biliary epithelial cells derived from small and large bile ducts. *Am J Physiol Gastrointest Liver Physiol* 299: G769–G777, 2010. First published June 24, 2010; doi:10.1152/ajpgi.00237.2010.— Biliary epithelial cells (BEC) are morphologically and functionally heterogeneous. To investigate the molecular mechanism for their diversities, we test the hypothesis that large and small BEC have disparity in their target gene response to their transcriptional regulator, the biliary cell-enriched hepatocyte nuclear factor HNF6. The expression of the major HNF (*HNF6*, *OC2*, *HNF1b*, *HNF1a*, *HNF4a*, *C/EBPb*, and *Foxa2*) and representative biliary transport target genes that are HNF dependent were compared between SV40-transformed BEC derived from large (SV40LG) and small (SV40SM) ducts, before and after treatment with recombinant adenoviral vectors expressing *HNF6* (AdHNF6) or control *LacZ* cDNA (AdLacZ). Large and small BEC were isolated from mouse liver treated with growth hormone, a known transcriptional activator of HNF6, and the effects on selected target genes were examined. Constitutive *Foxa2*, *HNF1a*, and *HNF4a* gene expression were 2.3-, 12.4-, and 2.6-fold, respectively, higher in SV40SM cells. This was associated with 2.7- and 4-fold higher baseline expression of HNF1a- and HNF4a-regulated *ntcp* and *oatp1* genes, respectively. Following AdHNF6 infection, *HNF6* gene expression was 1.4-fold higher ($P = 0.02$) in AdHNF6 SV40SM relative to AdHNF6 SV40LG cells, with a corresponding higher *Foxa2* (4-fold), *HNF1a* (15-fold), and *HNF4a* (6-fold) gene expression in AdHNF6-SV40SM over AdHNF6-SV40LG. The net effects were upregulation of HNF6 target gene *glucokinase* and of Foxa2, HNF1a, and HNF4a target genes *oatp1*, *ntcp*, and *mrp2* over AdLacZ control in both cells, but with higher levels in AdH6-SV40SM over AdH6-SV40LG of *glucokinase*, *oatp1*, *ntcp*, and *mrp2* (by 1.8-, 3.4-, 2.4-, and 2.5-fold, respectively). In vivo, growth hormone-mediated increase in *HNF6* expression was associated with similar higher upregulation of *glucokinase* and *mrp2* in cholangiocytes from small vs. large BEC. Small and large BEC have a distinct profile of hepatocyte transcription factor and cognate target gene expression, as well as differential strength of response to transcriptional regulation, thus providing a potential molecular basis for their divergent function.

heterogeneity; bile transport; hepatocyte nuclear factors; hepatocyte nuclear factor 6

HEPATIC GENE EXPRESSION IS primarily regulated at the transcriptional level by families of hepatocyte nuclear factors (HNF). Among these, the homeodomain HNF1, the orphan nuclear receptor HNF4, the ONECUT HNF6 (also known as OC-1 and OC-2), forkhead box (FoxA), and the CCATT/enhancer-binding proteins (C/EBP) are cell-autonomous, liver-enriched transcription factors bearing specific DNA-binding domains, which recognize cognate DNA motifs on the regulatory region of hepatic target genes to participate in a cross-regulatory network for modulating target gene activities (10, 36). In vivo, HNF participate in the liver developmental program. For instance, Foxa1 and Foxa2 are implicated in hepatic specification (24), HNF4a in hepatic fate determination (30), and OC1 and OC2 in biliary cell lineage specification (8). HNF also participate in the regulation of hepatic function in the mature liver, including glucose metabolism by HNF4a (39), HNF1a (25), HNF6 (22), or cholesterol and bile acid metabolism by HNF6 (41) and Foxa2 (7).

The liver is the largest internal organ of the body and is composed of two types of epithelial cells: *1*) hepatocytes and *2*) cholangiocytes (2). Hepatocytes account for ~70% and cholangiocytes for 3–5% of the endogenous liver cell population. Cholangiocytes [also known as biliary epithelial cells (BEC)] populate the bile ducts (2). The intrahepatic bile duct size ranges from large ducts emanating from the confluence of the extrahepatic bile ducts at the liver hilum to progressively smaller intrahepatic ducts (19). In experimental models, small BEC refer to BEC lining the small bile ducts, whereas large BEC line larger biliary ducts (3, 15). Small and large rodent BEC have distinct morphometry (15), gene expression profile (38), as well as proliferative, apoptotic, and secretory responses to experimental stimuli (1, 14, 15). This BEC heterogeneity is clinically relevant in that the large and small ducts are differentially targeted in human cholangiopathies (37), stressing the importance of understanding the molecular mechanism regulating their functional diversities.

Since hepatocytes and BEC embryonic cellular origins are from multipotent hepatoblasts (34), it is not surprising that they have overlapping physiological function, such as solute secretion and metabolic activities (23), and are, therefore, likely to share transcriptional regulation. Compared with BEC, the role of HNF in the molecular regulation of differentiated liver-specific genes in hepatocytes is better understood (10, 36). Among HNFs, the current body of data suggest that HNF6 is a dominant BEC-enriched transcription factor. It is critical to the early commitment of hepatoblasts to the biliary epithelial lineage as mutant mice with global HNF6 deletion exhibit biliary duct malformations and early mortality from cholestasis (9). Our laboratory has shown that HNF6 transcription factor is also highly expressed in BEC in the mature mouse liver and can negatively regulate BEC proliferation during early bile

* S. Glaser and M. Wang contributed equally to this work.

Address for reprint requests and other correspondence: A.-X. Holterman, RUSH Univ. Medical Center, Dept.s of Pediatrics and Surgery, 1725 W Harrison Str, Suite 718, Chicago, IL 60612 (e-mail: ai-xuan_holterman@rush.edu).

duct ligation injury (17). The transcriptional regulation of hepatic target genes by HNF6 is broad, involving gene with metabolic and transport function (22, 29, 35, 41), as well as other HNF, such as *HNF4a* (21), *HNF1b* (9), and *Foxa2* (21), suggesting that HNF6 can comprehensively regulate the biliary cell molecular signature, and that enforced HNF6 expression in large and small biliary cells would elucidate the molecular basis for their heterogeneity. To further our understanding of BEC gene regulation, we herein test the hypothesis that the biliary cell-enriched transcription factor HNF6 differentially regulates the large and small BEC downstream transcriptional events. We first characterized the expression profile of HNF and selected HNF target genes in the SV40 large T antigen-transformed and immortalized large and small BEC (SV40LG and SV40SM, respectively). We compared changes in the BEC transcriptional response to increasing HNF6 expression in these cell lines using recombinant adenoviral vectors expressing *HNF6* cDNA (AdHNF6). We evaluated representative in vivo HNF6 target gene expression in large and small BEC isolated from liver tissues following administration of HNF6-enhancing vector growth hormone (GH), a known STAT5-mediated transcriptional activator of HNF6 promoter (21).

MATERIALS AND METHODS

Materials. SV40LG and SV40SM BEC were derived from BALB/c mice and characterized as previously described (38). The construction and preparation of the replication-defective recombinant adenoviral vectors expression of the bacterial LacZ (AdLacZ) or mouse HNF6 cDNA (AdHNF6) have been reported (41). HNF6, HNF1a, HNF4a, Foxa2, C/EBPb, and β-actin antibodies were obtained from Santa Cruz Technology.

Cell culture. As previously described (15), cells were incubated at 37°C in 5% CO_2 atmosphere in D-MEM (Gibco) supplemented with 10% FBS, 1% pen/strep, and 1% L-glutamine. For experiments (n = 4), cells were plated at 5×10^6 cells in 10-cm culture dishes for mock infection or infection with a multiplicity of infection of 35 infectious units of AdHNF6 or AdLacZ in 1 ml of media for 60 min, following which media was added to a final 10-ml volume. Cells were harvested after 24 h of infection and washed three times with PBS to remove residual virus for subsequent total RNA extraction.

Animal procedures. Six- to eight-week-old male CD1 mice were kept in a 12:12-h light-dark-cycles with free access to standard chow and water. All animals received humane care, according to the criteria outlined in the Guide for the Care and Use of Laboratory Animals by the National Academy of Sciences and the National Institutes of Health (NIH). The animal care and use section of the NIH funding application was reviewed in accordance with the policies of the Institutional Animal Care and Use Committee and approved. Mice received an initial intraperitoneal injection of human recombinant GH (obtained from the National Institute of Diabetes and Digestive and Kidney Diseases National Hormone and Peptide Program) at 4 μg/g body wt, followed by a 3 μg/g body wt injection every 6 h and killed after 24 h for BEC isolation and purification.

BEC isolation. The procedure was described previously (2) but briefly, following in situ collagenase perfusion, in three different experiments, the cholangiocyte mixture from the biliary tracts were separated into large and small cells by counterflow elutriation (3) with further purification by immunoaffinity using immunomagnetic beads. Glucose-6-phosphatase and vimentin immunostaining was done to rule out contamination by hepatocytes and mesenchymal cells, respectively (1).

Gene analyses. Total liver RNA was extracted using RNA-STAT-60 (Tel-Test "B", Friendswood, TX). Following DNase I (Ambion, Austin, TX) digestion, cDNA was synthesized using the cDNA Synthesis Kit (Biorad, Hercules, CA) and purified through Qiagen column. Reactions were amplified using the appropriate primer sets and analyzed in triplicate using a MyiQ Single Color Real-Time PCR Detection System (Biorad). The relative expression of the genes was calculated by a mathematical delta-delta method developed by PE Applied Biosystems. Levels were reported after normalization to housekeeping gene cyclophilin for each gene. The primers sequences for mouse genes are provided in Table 1.

Western blot assays. Crude protein extracts were prepared from AdHNF-6 infected SV40LG and SV40SM cells, and protein concentrations were determined using the Bradford method (Bio-Rad). HNF6, HNF1a, HNF4a, Foxa2, C/EBPb, and β-actin immune complexes were detected with horseradish-conjugated secondary antibody (Fisher), followed by chemiluminescence (ECL + plus, Amersham Biosciences).

Statistical analysis. All data are expressed as means ± SD, unless otherwise indicated. Intergroup differences were evaluated by analysis of variance for repeated measures. A P value of <0.05 is considered to be significant. All statistical analyses were performed with the software SPSS.

RESULTS

Constitutive expression of hepatocyte transcription factors in SV40LG and SV40SM cells. The SV40 large T antigen-transformed large (SV40LG) and small BEC (SV40SM), derived from large and small bile ducts of mouse liver, were

Table 1. *Primer sequences for mouse genes*

Gene	Primers	
	Forward sequence	Reverse sequence
Transcription factors		
HNF1a	5′-TTC TAA GCT GAG CCA GCT GCA GAC G-3′	5′-GCT GAG GTT CTC CGG CTC TTT CAG A-3′
HNF1b	5′-GAA AGC AAC GGG AGA TCC TC-3′	5′-CCT CCA CTA AGG CCT CCC TC-3′
HNF6	5′-GGT CTG GGC AGC ATT CAC AAC-3′	5′-CAG GGT GGT GGG CTT CAA AG-3′
HNF4a	5′-ACA CGT CCC CAT CTG AAG-3′	5′-CTT CCT TCT TCA TGC CAG-3′
C/EBPb	5′-ATC GAC TTC AGC CCC TAC CT-3′	5′-GGC TCA CGT AAC CGT AGT CG-3′
Foxa2	5′-CCA TCA GCC CCA CAA AAT G-3′	5′-CCA AGC TGC CTG GCA TG-3′
Hepatic function genes		
Glucokinase	5′-CCT GGG CTT CAC CTT CTC CTT-3′	5′-GAG GCC TTG AAG CCC TTG GT-3′
Mrp2	5′-AGA GGG CGG TGA CAA CCT GAG-3′	5′-CGG ATG GTC GTC TGA ATG AGG-3′
Ntcp	5′-ATG ACC ACC TGC TCC AGC TT-3′	5′-GCC TTT GTA GGG CAC CTT GT-3′
Oatp1	5′-AAT TTG GGA AGA GTG GCC TT	5′-TGG AGT CAA TGC AAA AAC CA
TGFb2R	5′-CGG AAA TTC CCA GCT TCT GG-3′	5′-TTT GGT AGT GTT CAG CGA GC-3′

Sequences are annotated with the binding position upstream of the transcription start site. See text for definitions of gene acronyms.

previously characterized (38) and shown to display morphological, phenotypic, and functional characteristics of freshly isolated large and small cholangiocytes (15). The baseline profile in the expression of hepatocyte transcription factors *HNF6* (*OC1*) and its paralog *OC2* (18), *HNF1b*, *HNF1a*, *HNF4a*, *Foxa2*, and *C/EBPb* was assessed by real-time PCR in SV40LG and SV40SM cell lines. Figure 1 illustrates that, while *HNF6*, *OC2*, *HNF1b*, and *C/EBPb* gene expression levels were comparable in small and large BEC, *Foxa2*, *HNF1a*, and *HNF4a* levels were 2.3-fold (P = 0.001), 12.4-fold (P = 0.001), and 2.6-fold (P = 0.02), respectively, higher in SV40SM cells. Consistent with the fact that HNF expression is primarily regulated at the transcriptional level, Western blotting for protein expression (Fig. 1*B*) exhibits the same pattern of higher *Foxa2*, *HNF1a*, and *HNF4a* levels in SV40SM cells.

Constitutive expression of HNF target genes in SV40LG and SV40SM cells. Intrahepatic bile acid transport is among many of BEC important functions (26). We next examined the expression of hepatic bile acid transport genes, which are known target genes for HNF: *ntcp* (the Na^+-dependent taurocholate cotransport peptide for bile acid import, also known as slc10a1) is transcriptionally regulated by *HNF1a* (13) and *HNF4a* (13, 16); *mrp2* (the multidrug resistance-associated protein for xeno- and endobiotics bile acid export, also known as abcc2) by *HNF1a* and *HNF4a* (20, 32), and possibly by *Foxa2* (7); and *oatp1* (the organic anion transporter for basolateral bile acid uptake, also known as slc21a1) by *HNF1a* (4, 27) and *HNF4a* (11, 16). Since the above data showed that SV40LG and SV40SM cells have differential expression of *Foxa2*, *HNF1a*, and *HNF4a* transcription factors, we next sought to characterize the baseline expression of *HNF6*, *Foxa2*, *HNF1a*, and *HNF4a* target genes. As control target genes for *HNF6*, we assayed *glucokinase* (*GK*, previously shown to be positively regulated by HNF6) (22) and *TGFb2R* (shown to be negatively regulated by HNF6) (31, 40) and did not find differences in their baseline expression (Fig. 2). HNF1a/HNF4a target genes *ntcp* and *oatp1* are expressed at 2.7-fold (P = 0.004) and 4-fold higher levels (P = 0.01) in SV40SM than SV40LG cells. Since *mrp2* expression levels were low, the biological significance of a statistical difference in the expression between SV40LG and SV40SM cells (1.6-fold higher in SV40SM, P = 0.001) is not clear.

Effects of increasing HNF6 expression in BEC on known HNF6 target genes. Since HNF6 is a major BEC-enriched transcription factor, cells were mock infected or treated with AdLacZ and AdHNF6 to assess if increasing HNF6 expression can transcriptionally alter BEC gene profiles. Since mock-infected cells have comparable gene expression levels as AdLacZ-infected cells (data not shown), the results comparing AdLacZ- against AdHNF6-infected cells are presented (Table 2). Previous studies have shown that AdHNF6 tail vein injection effectively increased *HNF6* gene and nuclear protein expression in both hepatocytes and bile ducts (17). Following AdHNF6 treatment, *HNF6* gene expression was also appropriately increased in AdHNF6-SV40LG and AdHNF6-SV40SM cells relative to AdLacZ-treated control by 1,450-fold and 2,608-fold, respectively, corresponding to a 1.4-fold higher HNF6 expression in AdHNF6-SV40SM relative to AdHNF6-SV40LG (P = 0.02) (Table 1). Western blotting of AdLacZ- and AdHNF6-infected SV40LG and SV40SM cells confirmed a similar pattern of higher HNF6 protein expression in AdHNF6-SV40SM cells (Fig. 3). HNF6 target gene *TGFb2R* (Table 2) changed minimally in AdHNF6-infected SV40LG, but, con-

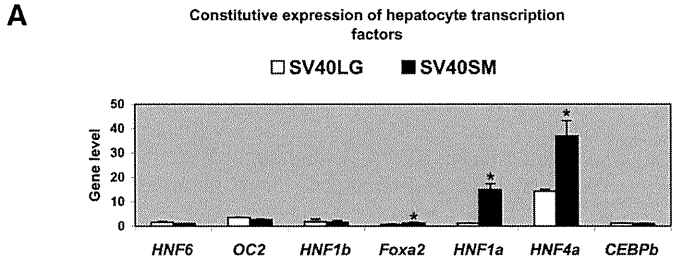

Genes	Cells SV40 LG	Cells SV40 SM	x-fold gene levels SV40SM over SV40LG	p value
Foxa2	0.56 +/- 0.3	13 +/- 0.2	**2.3***	**0.001**
HNF1a	1.2 +/- 0.1	14.9 +/- 2.5	**12.4***	**0.001**
HNF4a	14.3 +/- 1.4	36.9 +/- 6.3	**2.6***	**0.02**

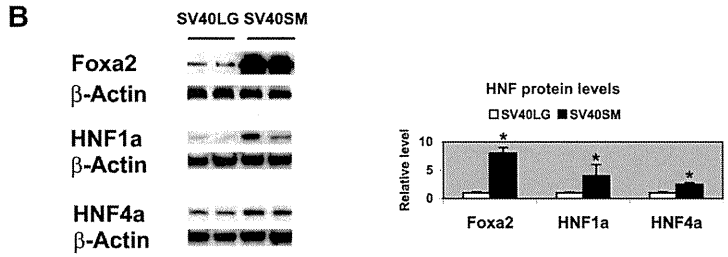

Fig. 1. Constitutive expression of hepatocyte transcription factors in SV40LG (large) and SV40SM (small) cell lines. *A*: real-time PCR bar graph of *HNF6*, *OC2*, *HNF1a*, *HNF1b*, *Foxa2*, *HNF4a*, and *C/EBPb* gene levels (after normalization to housekeeping gene *cyclophilin*), showing higher *Foxa2*, *HNF1a*, and *HNF4a* in SV40SM over SV40LG cells. The table shows *Foxa2*, *HNF1a*, and *HNf4a* gene levels and the x-fold higher expression with the corresponding P values in SV40SM over SV40LG cells. *B*: Western blotting micrographs of Foxa2, HNF1a, HNF4a, and β-actin protein expression in SV40LG and SV40SM cells. Bar graph of densitometry analysis of the immune complexes after normalization with β-actin shows higher Foxa2, HNF1a, and HNF4a expression levels in SV40SM cells relative to SV40LG cells. *P values of significance at <0.05. See text for definitions of gene acronyms used in figures.

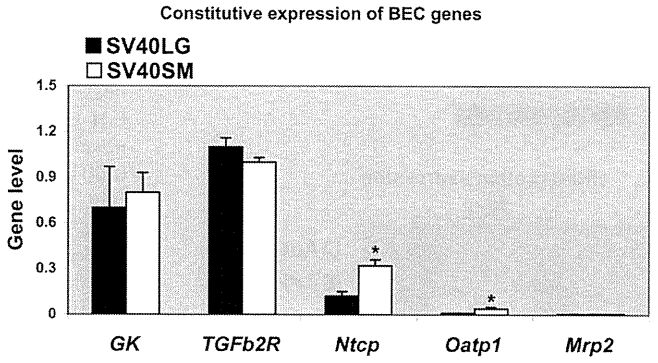

Fig. 2. Constitutive expression of target genes in SV40LG and SV40SM cell lines. Real-time PCR bar graph shows *glucokinase* (*GK*), *TGFb2R*, *ntcp*, *oatp1*, and *mrp2* gene levels, and table shows *ntcp*, *oatp1a1*, and *mrp2* gene levels and the x-fold higher expression in SV40SM over SV40LG cells with the corresponding *P* values. *Significant *P* values.

Genes	Cells SV40 LG	Cells SV40 SM	x-fold gene levels SV40SM over SV40LG	p value
GK	0.7 +/- 0.27	0.8 +/- 0.13	1.1	0.5
TGFb2R	1.1 +/- 0.06	1 +/- 0.03	1	0.7
Ntcp	0.12 +/- 0.03	0.32 +/- 0.04	**2.7***	**0.004**
Oatp1	0.01 +/- 0.001	0.04 +/- 0.01	**4***	**0.01**
Mrp2	0.001 +/- 0.001	0.0016 +/- 0.001	(1.6)	(0.001)

sistent with the higher expression of *HNF6* in AdHNF6-SV40SM cells, its level is 1.6-fold more diminished in AdHNF6-SV40SM relative to AdHNF6-SV40LG cells (P = 0.03). HNF6 target gene *glucokinase* response was more dramatic, with a 16- and 38-fold upregulation following AdHNF6 infection over AdLacZ control in AdHNF6-SV40LG and AdHNF6-SV40SM cells, respectively, corresponding to an 1.8-fold higher (P = 0.02) *glucokinase* expression in AdHNF6-SV40SM cells compared with AdHNF6-SV40LG cells. These results demonstrate that BEC and hepatocytes display similar HNF6 target gene response, but most of all, that small BEC have higher reactivity to HNF6 transcriptional regulation.

Effects of increasing HNF6 BEC expression on other HNF and HNF-regulated bile transport target genes. We next evaluated the effect of HNF6 overexpression on the transcriptional response of other known HNF6-dependent HNF [such as *HNF4a* (21), *HNF1b* (9), and *Foxa2* (21)] in BEC (Fig. 4). Despite an unexpected AdHNF6-associated suppression of endogenous HNF4a gene levels (Fig. 4*B*) in both SV40SM (by 2-fold, P = 0.05) and SV40LG cells (by 6.4-fold, P = 0.002), the net effect of higher *HNF6* expression in AdHNF6-SV40SM over AdHNF6-SV40LG BEC is illustrated in Fig. 4*A*, demonstrating that the final *Foxa2*, *HNF1a*, and *HNF4a* expression in AdHNF6-infected small BEC remained markedly higher than in AdHNF6-infected large BEC, with a 4-fold (P = 0.01), 15-fold (P = 0.001), and 6.5-fold (P = 0.03) difference, respectively.

Effects of AdHNF6 treatment on HNF-regulated bile transport target genes. As seen in Fig. 5, the response to AdHNF6 infection in both SV40LG and SV40SM cells of the biliary genes was characterized in AdHNF6-SV40 cells relative to AdLacZ-SV40 cells by upregulation of *ntcp*, *oatp1*, and *mrp2* expression with enhanced *ntcp* (5.3-fold up, P = 0.001, Fig. 5*A*), *oatp1* (5-fold up, P = 0.001, Fig. 5*B*), and *mrp2* (24-fold up, P = 0.01, Fig. 5*C*) expression in AdHNF6-SV40 LG cells, and increased *ntcp* by 6.5-fold (P = 0.001, Fig. 5*A*), *oatp1* by 4.2-fold (P = 0.003, Fig. 5*B*), and *mrp2* by 30-fold (P = 0.001, Fig. 5*C*) in AdHNF6-SV40SM cells.

The net effects of AdHNF6 infection of higher *HNF6*, *Foxa2*, *HNF1a*, and *HNF4a* expression in AdHNF6-SV40SM relative to AdHNF6-SV40LG were associated with correspondingly higher levels of *ntcp* (2.4-fold, P = 0.02), *oatp1*

Table 2. *Effect of AdHNF6 on HNF6 and HNF6 target genes*

	AdLacZ	AdH6	x-Fold AdHNF6 vs. AdLacZ	x-fold AdHNF6 SV40SM vs. AdHNF6 SV40LG	*P* Value
HNF6					
SV40LG	0.7 ± 0.3	725 ± 109	1,450		
SV40SM	0.4 ± 0.3	1043 ± 98	2,608	1.4	0.02
GK					
SV40LG	0.8 ± 0.37	13 ± 1.9	16		
SV40SM	0.6 ± 0.2	23 ± 4.6	38	1.8	0.02
TGFb2R					
SV40LG	1 ± 0.14	0.8 ± 0.1	0.8		
SV40SM	1 ± 0.11	0.5 ± 00.1	2.0	1.6	0.03

SV40LG and SV40SM cells were treated with AdLacZ or AdHNF6 for 24 h. Total RNA was extracted for real-time PCR analysis of *HNF6*, *cyclophilin*, and HNF6-target genes *glucokinase (GK)* and *TGFb2R*. Table shows gene levels after normalizing with housekeeping gene *cyclophilin*, the x-fold changes in gene level between AdLacZ-treated cells and AdHNF6-treated cells, and the x-fold difference between AdHNF6-treated SV40SM and AdHNF6-treated SV40LG cells with its corresponding *P* values. See text for definitions of gene acronyms.

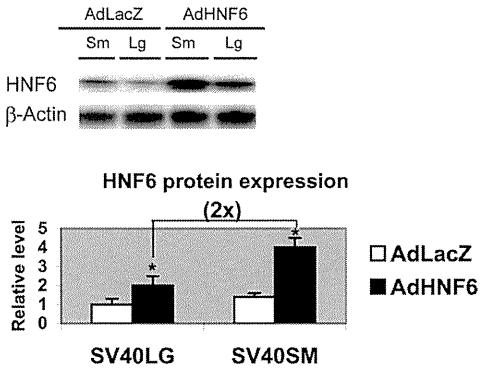

Fig. 3. Effect of adenoviral HNF6 (AdHNF6) treatment on SV40 biliary epithelial cell (BEC) HNF6 protein expression. SV40LG and SV40SM cells were infected with AdLacZ and AdHNF6 for 24 h. Micrograph shows Western blotting results of HNF6 protein expression in SV40SM (Sm) and SV40LG (Lg) cells. Bar graph shows densitometry results of the immune complexes after normalization to β-actin with values reported relative to AdHNF6-infected SV40LG cells, showing a twofold higher HNF6 expression in AdHNF6-SV40SM over AdHNF6-SV40LG cells. *Significant P values.

(3.4-fold, $P = 0.006$), and *mrp2* (2.5-fold, $P = 0.02$) in AdHNF6-SV40SM compared with AdHNF6-SV40LG cells.

Effects of increasing in vivo HNF6 expression on target gene transcription. To evaluate HNF6 in vivo target gene transcriptional response, hepatic HNF6 expression was physiologically enhanced by treatment with recombinant GH, a known STAT5-mediated transcriptional activator of HNF6 promoter (21). The *mrp2* gene expression was selected since, among the above bile transport gene-positive transcriptional responses to AdHNF6 treatment, *mrp2* levels were the most dramatically enhanced (by >20-fold in both SV40LG and SV40SM cells). Large and small BEC were isolated for gene expression analyses following 24 h of GH administration (Fig. 6). As expected from our laboratory's previous work in GH-treated liver (40, 41), *HNF6* gene expression was appropriately increased in large (by 1.5-fold) and small BEC (by 1.7-fold) relative to PBS control (Fig. 6*A*). Consistent with our laboratory's previous findings that SV40SM cell lines displayed a magnified responsiveness to HNF6 induction relative to SV40LG cells, in vivo GH-treated small BEC had significant increases of *glucokinase* (2.8-fold, $P = 0.05$; Fig. 6*B*) and *mrp2* (5-fold, $P < 0.001$; Fig. 6*A*) gene expression over PBS-treated small BEC. Of note, unlike our laboratory's previous SV40 cell data showing enhanced *glucokinase* (Table 1) and *mrp2* response (Fig. 5*C*) to AdHNF6 infection in SV40LG cells, this increase was not seen in GH-treated large BEC, possibly because GH-induced *HNF6* in vivo expression was less dramatic. Compared with GH-treated large BEC, *glucokinase* and *mrp2* levels were 2.4-fold ($P = 0.04$) and 3.4-fold ($P < 0.001$), respectively, higher in GH-treated small BEC than GH-treated large BEC, showing that the same pattern of small BEC in vitro sensitivity in its transcriptional response to HNF6 was also seen in vivo.

DISCUSSION

The concept of biliary cell morphological and functional heterogeneity originating from the early work in rat biliary model system (2, 6) has progressively gained acceptance with many comprehensive reviews on this subject (14, 19, 28). Since the liver epithelial cell phenotype and function are determined by the spectrum of hepatic-specific genes, whose expression are regulated by liver-enriched HNFs, an evaluation of the BEC transcriptional characteristics is a logical start in furthering our understanding of basic molecular mechanism for BEC diversities.

We found that the small and large BEC display distinctive constitutive levels of hepatocyte transcription factors and biliary cell-enriched gene expression. The small SV40 BEC exhibited higher expression of *Foxa2*, *HNF1a*, and *HNF4a* hepatocyte transcription factors. This transcriptional profile likely provides the molecular basis for higher constitutive expression of HNF1a-, HNF4a-, and Foxa2-candidate target genes such as *ntcp*, *oatp1*, and *mrp2* in SV40SM cells. The

A

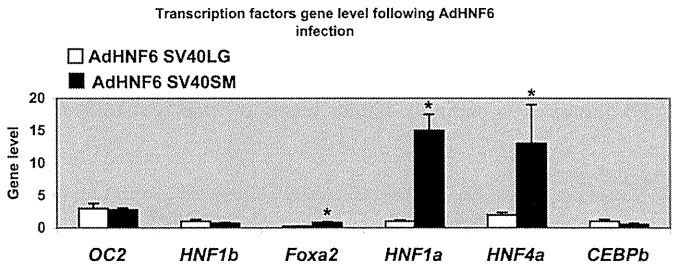

Genes	Cells AdHNF6 SV40LG	Cells AdHNF6 SV40SM	x-fold gene levels SV40SM over SV40LG	p value
HNF1a	1 +/- 0.2	15 +/- 2.5	**15***	**0.001**
HNF4a	2 +/- 0.38	13 +/- 6	**6.5***	**0.03**
Foxa2	0.2+/- 0.04	0.8 +/- 0.1	**4***	**0.01**

B

HNF4a	AdLacZ	AdHNF6	x-fold suppression	p value
SV40 LG	11.8 +/- 1.3	2 +/- 0.38	**6.4***	**0.002**
SV40 SM	31 +/- 7.2	13 +/- 6	**2***	**0.05**

Fig. 4. Net effect of AdHNF6 treatment on SV40 BEC hepatocyte nuclear factor (HNF) expression. *A*: bar graph shows *OC2*, *HNF1b*, *Foxa2*, *HNF1a*, *HNF4a*, *and C/EBPb* gene levels for AdHNF6-infected SV40LG and AdHNF6-infected SV40SM cells. *Significant differences in levels between AdHNF6 SV40LG vs. AdHNF6 SV40SM cells. Table shows gene levels and the x-fold higher expression levels of *HNFa1*, *HNF4a*, and *Foxa2* in AdHNF6-SV40SM relative to AdHNF6-SV40LG cells with the corresponding P values. *B*: table shows *HNF4a* gene levels in AdLacZ- and AdHNF6-infected SV40LG and SV40SM cells and x-fold suppression (with the corresponding P values) in gene levels of AdHNF6-infected SV40 cells relative to AdLacZ-infected cells. *Significant differences in levels between AdLacZ and AdHNF6-infected cells.

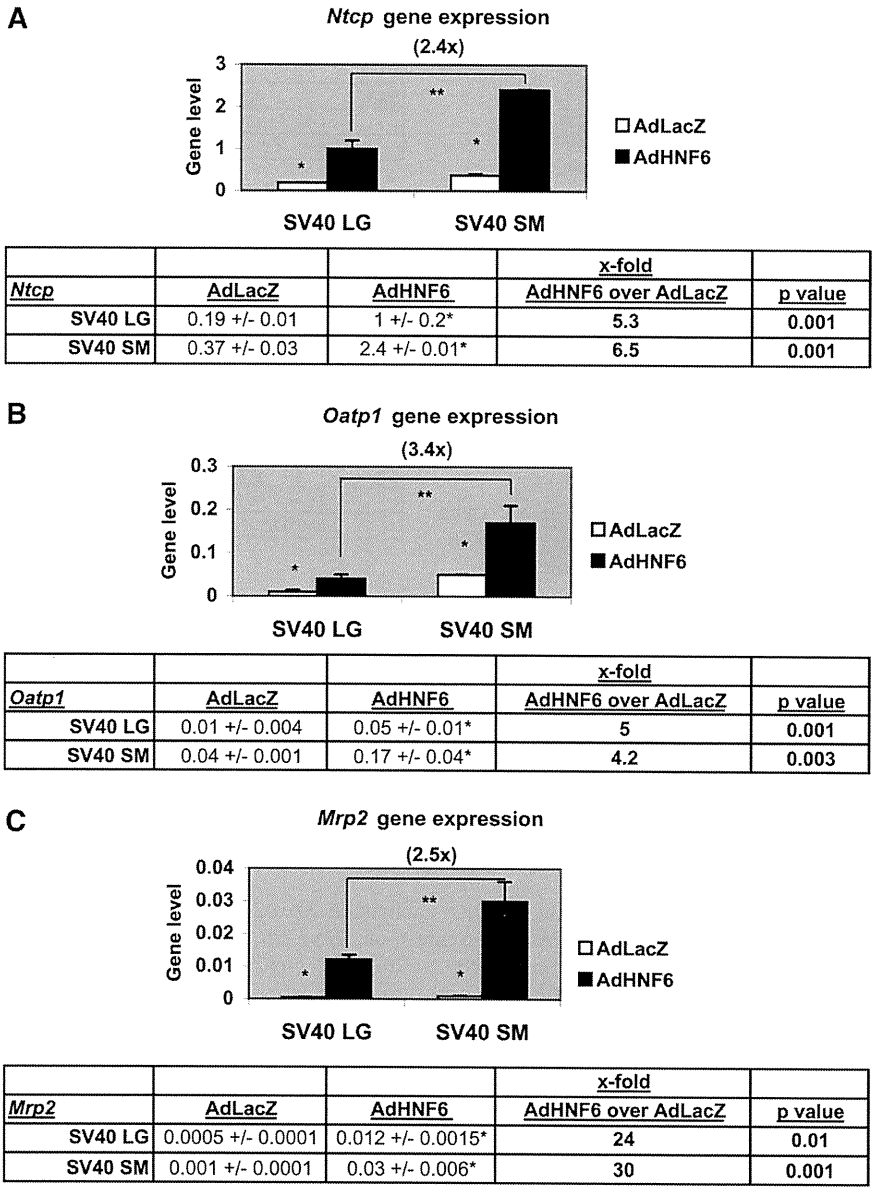

			x-fold	
Ntcp	AdLacZ	AdHNF6	AdHNF6 over AdLacZ	p value
SV40 LG	0.19 +/- 0.01	1 +/- 0.2*	5.3	0.001
SV40 SM	0.37 +/- 0.03	2.4 +/- 0.01*	6.5	0.001

			x-fold	
Oatp1	AdLacZ	AdHNF6	AdHNF6 over AdLacZ	p value
SV40 LG	0.01 +/- 0.004	0.05 +/- 0.01*	5	0.001
SV40 SM	0.04 +/- 0.001	0.17 +/- 0.04*	4.2	0.003

			x-fold	
Mrp2	AdLacZ	AdHNF6	AdHNF6 over AdLacZ	p value
SV40 LG	0.0005 +/- 0.0001	0.012 +/- 0.0015*	24	0.01
SV40 SM	0.001 +/- 0.0001	0.03 +/- 0.006*	30	0.001

Fig. 5. Effect of AdHNF6 treatment on SV40 BEC gene expression. SV40LG and SV40SM cells were infected with AdLacZ and AdHNF6 for 24 h. Bar graphs show gene levels for *ntcp* (*A*), *oatp1* (*B*), and *mrp2* (*C*) in AdLacZ- and AdHNF6-infected SV40LG and SV40SM cells. *Significant differences in levels between AdLacZ and AdHNF6-infected cells. **Significantly higher *ntcp*, *oatp1*, and *mrp2* levels (2.4-, 3.4-, and 2.5-fold, respectively) in AdHNF6-infected SV40SM cells compared with AdHNF6-infected SV40LG. The tables show gene levels of infected cells with the corresponding *P* values.

dominance of *HNF1a* and *HNF4a* as BEC-enriched transcription factors in small biliary cells is consistent with previous genomewide promoter analyses of human hepatocytes, showing that *HNF1a*, *HNF4a*, and *HNF6* are the core group of HNFs in orchestrating the transcription of a wide array of differentiated hepatic genes (29). Of great interest to us, it remains to be seen in future experiments whether large biliary cell could be induced into acquiring the same small BEC molecular repertoire upon enforced expression of these HNF1a-, HNF4a-, and Foxa2-enriched hepatocyte transcription factors, and, conversely, whether the small biliary cell would lose its constitutive molecular imprint following reversal of its HNF profile.

Small BEC also displayed a higher transcriptional response level to HNF6 treatment. Since HNF6 transcriptional regulation of target gene also involves other HNF, such as *HNF4a* (21), *HNF1b* (9), and *Foxa2* (21), we first evaluated HNF response patterns to AdHNF6 in SV40 BEC. Consistent with the known cross-regulatory transcriptional network among HNFs, AdHNF6 treatment affected the HNF profile of BEC, albeit with a negative effect on *HNF4a* transcription for both large and small SV40 BECs. A simple explanation for this unexpected suppressive response is that previous results demonstrating hepatic HNF4a-positive transcriptional response to HNF6 could not be extrapolated to that of BEC. Alternatively, the approach of using HNF6 adenoviral expression vectors to transduce HNF6 expression in BEC cell lines limits this analysis to HNFs as cell-autonomous regulators outside the context of in vivo systems. An evaluation of in vivo cholangiocytes' HNF and